

Original Article

A chemical biology approach identified PI3K as a potential therapeutic target for neurofibromatosis type 2

Alejandra M Petrilli¹, Marisa A Fuse¹, Mathew S Donnan¹, Marga Bott¹, Nicklaus A Sparrow¹, Daniel Tondera^{3,4}, Julia Huffziger³, Corina Frenzel³, C Siobhan Malany², Christophe J Echeverri³, Layton Smith², Cristina Fernández-Valle¹

¹Burnett School of Biomedical Sciences, College of Medicine, University of Central Florida, Florida, U.S.A.; ²Drug Discovery and Pharmacology, Conrad Prebys Center for Chemical Genomics, Sanford-Burnham Medical Research Institute, Orlando-Lake Nona, Florida, U.S.A.; ³Cenix BioScience GmbH, Dresden, Germany; ⁴Current affiliation: Silence Therapeutics, Berlin, Germany

Received June 20, 2014; Accepted August 16, 2014; Epub October 11, 2014; Published October 15, 2014

Abstract: Mutations in the merlin tumor suppressor gene cause Neurofibromatosis type 2 (NF2), which is a disease characterized by development of multiple benign tumors in the nervous system. The current standard of care for NF2 calls for surgical resection of the characteristic tumors, often with devastating neurological consequences. There are currently no approved non-surgical therapies for NF2. In an attempt to identify much needed targets and therapeutically active compounds for NF2 treatment, we employed a chemical biology approach using ultra-high-throughput screening. To support this goal, we created a merlin-null mouse Schwann cell (MSC) line to screen for compounds that selectively decrease their viability and proliferation. We optimized conditions for 384-well plate assays and executed a proof-of-concept screen of the Library of Pharmacologically Active Compounds. Further confirmatory and selectivity assays identified phosphatidylinositol 3-kinase (PI3K) as a potential NF2 drug target. Notably, loss of merlin function is associated with activation of the PI3K/Akt pathway in human schwannomas. We report that AS605240, a PI3K inhibitor, decreased merlin-null MSC viability in a dose-dependent manner without significantly decreasing viability of control Schwann cells. AS605240 exerted its action on merlin-null MSCs by promoting caspase-dependent apoptosis and inducing autophagy. Additional PI3K inhibitors tested also decreased viability of merlin-null MSCs in a dose-dependent manner. In summary, our chemical genomic screen and subsequent hit validation studies have identified PI3K as potential target for NF2 therapy.

Keywords: Neurofibromatosis type 2, phenotypic high-throughput screen, PI3K, PI3K inhibitor, apoptosis, autophagy

Introduction

Neurofibromatosis type 2 (NF2) is a tumor disorder of the nervous system caused by loss-of-function mutations in the Neurofibromatosis 2 gene (*NF2*) [1-3]. NF2 patients develop cranial and peripheral nerve schwannomas, meningiomas, and ependymomas [4]. Despite the benign nature of the tumors, their localization within the nervous system causes serious neurological symptoms and can be life threatening. Loss of hearing resulting from growth of bilateral vestibular schwannomas is typically the first symptom [4]. The *NF2* gene encodes merlin, a tumor suppressor protein. Merlin is a

member of the band 4.1 family of proteins that link cell surface glycoproteins to the cortical actin cytoskeleton [5]. Merlin modulates activity of numerous signaling pathways that regulate cell size, morphology, proliferation, and survival [6]. Although understanding of merlin-dependent signaling pathways continues to increase, there are currently no standard chemotherapeutic options for NF2 patients. NF2 patients typically undergo microsurgery or radiosurgery; however, the former leads to loss of nerve function when tumors are operable and the latter carries the risk of future malignant transformation of remaining tumor cells.

High-throughput screening (HTS) of compound libraries with phenotypic assays is an important strategy because it facilitates an unbiased chemical genomic approach to drug discovery and target identification. To that end, we created and optimized a merlin-null mouse Schwann cell (MSC) line for HTS. These cells were derived from primary Schwann cells (SCs) isolated from homozygous *Nf2^{fllox2/fllox2}* mice [7] by *in vitro* deletion of the *Nf2* exon 2 using Adeno-Cre-mediated recombination. Work in our laboratory and others has shown that the absence of exon 2 in merlin promotes its rapid proteosomal degradation, thereby creating functionally merlin-null MSCs [8-10]. Using these cells, we screened the Library of Pharmacologically Active Compounds (LOPAC, Sigma-Aldrich, St. Louis, MO) for compounds that decreased the viability of merlin-null MSCs. Follow-up confirmation, selectivity counter-screens, and dose-response experiments identified the class I phosphoinositide 3-kinase (PI3K) inhibitor AS-605240, (Z)-5-(quinoxalin-6-ylmethylene)thiazolidine-2, 4-dione, as an NF2 lead compound.

Merlin has been shown to inhibit PI3K activity by binding to phosphatidylinositol 3-kinase enhancer-L (PIKE-L), which disrupts binding of PIKE-L to PI3K [11]. PIKE-L is a GTPase that binds to PI3K and stimulates its lipid kinase activity [12]. In addition, loss of merlin leads to activation of the PI3K/Akt pathway in human schwannomas and subsequent proliferation and growth of the SCs [13]. Altered PI3K activity is implicated in various diseases including cancer, and PI3K mutations have been observed in various human solid tumors [14-16]. PI3K is a lipid kinase that phosphorylates phosphatidylinositol (3,4)-bisphosphate (PIP2) to produce phosphatidylinositol (3,4,5)-trisphosphate (PIP3). PI3K-dependent pathways regulate cell proliferation and survival in response to extracellular signaling primarily through receptor tyrosine kinases, integrins, cytokine receptors, and G-protein coupled receptors [14, 17]. The class I PI3-kinases are heterodimers consisting of a p110 catalytic subunit in complex with a p85 or p101 regulatory subunit. There are four different isoforms of catalytic p110 subunits: alpha, beta, gamma, and delta. The α and β isoforms of p110 are expressed in all cell types, whereas the γ and δ

isoforms are enriched in hematopoietic cells [15, 18-20]. In recent years, several small molecule PI3K inhibitors have been developed, and no less than fifteen compounds have progressed to clinical trials for cancer [21].

In summary, we conducted the first chemical genomic screen that successfully identified potential therapeutic targets and small molecule inhibitors for NF2. Confirmatory orthogonal and selectivity assays identified PI3K as an NF2 target. In addition, the PI3K inhibitor AS605240 selectively decreased merlin-null MSCs viability in a dose-dependent manner through a caspase-dependent apoptotic mechanism accompanied by induction of autophagy. Finally, nine other small-molecule PI3K and dual PI3K/mTOR inhibitors promoted similarly strong loss of viability of merlin-null MSCs.

Materials and methods

Materials

Adenovirus-expressing Cre recombinase gene (Ad5CMV-Cre) was purchased from Gene Transfer Vector Core (University of Iowa). The LOPAC@1280 library and the individual compounds re-tested, E64d and pepstatin A, were purchased from Sigma-Aldrich (St. Louis, MO, USA). Rapamycin and staurosporine were purchased from Santa Cruz Biotechnology (Santa Cruz, CA, USA). Digitonin was purchased from EMD chemicals (Billerica, MA, USA). Z-VAD-FMK (caspase-1, -4, -3 and -7 inhibitor) was purchased from Promega (Madison, WI, USA). GSK-2126458, PIK-75, CH-5132799, IC-87-114, XL-765, BEZ235, and CUDC 907 were purchased from Selleck Chemicals (Selleckchem.com Europe).

Antibodies

Merlin (D1D8) rabbit mAb, Akt rabbit Ab, phospho-Akt (T308) rabbit Ab, LC3B (D11) XP rabbit mAb, and β -Actin (8H10D10) mouse mAb were purchased from Cell Signaling (Danvers, MA, USA). Merlin C18 rabbit Ab was purchased from Santa Cruz Biotechnologies (Dallas, TX, USA). S-100 rabbit Ab was purchased from Dako Cytomation (Glostrup, Denmark). Secondary antibodies, goat anti-mouse- and goat anti-rabbit- IgG horseradish peroxidase conjugated, were purchased from Pierce/Thermo Fisher Scientific (Rockford, IL, USA). Goat anti-rabbit

IRDye 800CW and goat anti-mouse IRDye 680LT were purchased from LI-COR Odyssey (Lincoln, Nebraska USA). Goat anti-mouse IgG Alexa Fluor568 conjugated and goat anti-rabbit-IgG Alexa Fluor488 conjugated were purchased from Invitrogen (Grand Island, NY, USA).

Creation and culturing of merlin-null ($Nf2^{ex2/-}$) mouse Schwann cells

All dissections were performed following protocols approved by the University of Central Florida (UCF) Institutional Animal Care and Use Committee (IACUC) and animals were maintained in UCF's Vivarium that is certified by the International Association for Assessment and Accreditation of Laboratory Animal Care (AAALAC). SCs were isolated from sciatic nerves of 3-6 week-old homozygous $Nf2^{flox2/flox2}$ mice. Primary $Nf2^{flox2/flox2}$ SCs were purified and expanded for two passages in growth medium: DMEM/F12 1:1 (Gibco), 1x N2 supplement (Invitrogen), 2 μ M forskolin (Sigma), 10 ng/ml neuregulin (Recombinant Human NRG1 Isoform SMDF; R & D Systems), and 1% Penicillin/Streptomycin (Gibco), on 200 μ g/ml Poly-L-lysine hydrobromide (PLL; Sigma-Aldrich), 20 μ g/ml Laminin (Invitrogen) coated tissue culture plates (Corning). $Nf2^{flox2/flox2}$ SCs were transduced overnight with Adeno-Cre virus at 250 multiplicity of infection (MOI) when cultures reached ~70% confluency. The transduced cell population was expanded and deletion of $Nf2$ exon 2 was verified by PCR analysis of genomic DNA and merlin western blots. Merlin-null MSCs were cultured in CellBIND-Corning 100 mm dishes in their growth medium: DMEM/F12 1:1 (Gibco), 1X-N2 supplement (Invitrogen), and 1% penicillin/streptomycin (Gibco).

Western blots

Cultured $Nf2^{flox2/flox2}$ SCs and merlin-null MSCs were lysed in modified RIPA buffer (25 mM Tris-HCl, pH 7.6; 150 mM NaCl; 1% Triton X-100; 1% sodium dodecyl sulfate with protease inhibitor cocktail and phosphatase inhibitor cocktail 2 and 3; Sigma-Aldrich), as previously described [22]. Protein concentration was determined with the DC Assay (BioRad, Hercules, CA, USA) to load 10 μ g of protein per lane. To prepare whole cell extracts to study autophagy, merlin-null MSCs were lysed in 180 μ l of 2% SDS Loading buffer plus 2.5 U/ml benzonase, heat-

ed at 97°C for 5 minutes, and immediately loaded into 4-20% polyacrylamide gels (Pierce/Fisher Scientific). Resolved proteins in the gel were transferred to a PVDF membrane (Immobilon-P or Immobilon-FL, Millipore, Bedford, MA) and blocked with 5% BSA or Odyssey blocking buffer before blotting with primary antibodies and corresponding secondary antibodies conjugated with horse radish peroxidase or IRDye. Densitometric quantification of western blots was performed with NIH ImageJ software or Odyssey software.

Immunostaining

Control and merlin-null MSCs were seeded on 200 μ g/ml poly-L-lysine hydrobromide (Sigma-Aldrich) and 10 μ g/ml laminin-coated German glass coverslips. Immunostaining was performed as previously described [23]. Confocal images were acquired with a Zeiss LSM710 microscope with 3 spectral detection channels, 5 laser lines (458, 488, 514, 543, and 633 nm), and the EC Plan-Neofluar 40x/1.3 DIC WD=0.21 M27 objective lens on an Axio Observer Z1 Stand and ZEN2009 software.

Cell viability assays

Cell viability was assessed with two different assays, the MultiTox-Fluor Multiplex Cytotoxicity Assay (Promega) and the CellTiter-Glo assay (Promega). Control and merlin-null MSCs were seeded at 5,000 cells/well in 20 μ l phenol-red free growth media in 384-well CellBIND plates, centrifuged 1 min at 500 rpm, and briefly incubated at 37°C, 7% CO₂ for several hours to ensure cell attachment prior to compound treatment. Then, 5 μ l of compound/vehicle solution was added to each well, centrifuged 1 min at 500 rpm, and returned to incubation for 24 hrs. Cell viability assays were performed following manufacturer's specifications. Fluorescence measurement for the LOPAC screen was performed using EnVision (PerkinElmer) or the Synergy H1 Hybrid plate reader (BioTek, Winooski, VT, USA), Ex: 405 nm/Em: 492 nm for live cells and Ex: 485 nm/Em: 535 nm for dead cells. Luminescence was measured in a Synergy H1 Hybrid plate reader.

Caspase 3/7 activity assay

Merlin-null MSCs were seeded in 384-well Corning CellBIND plates at 5,000 cells/well in

PI3K as a pharmacological target in NF2

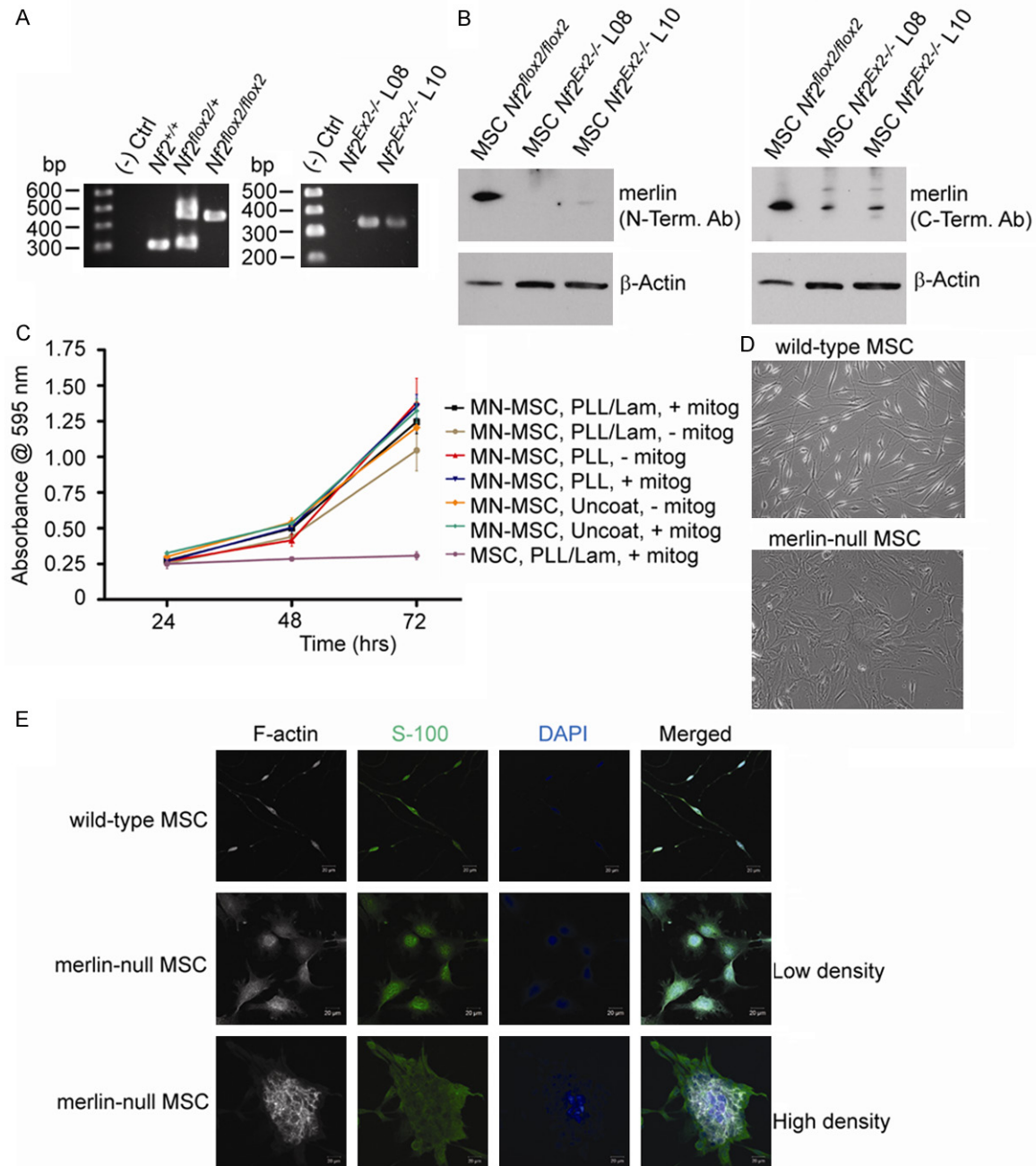


Figure 1. Creation and Characterization of Merlin-Null Mouse Schwann Cells. A. PCR amplification with primer set P4/5 produces 305 bp band indicative of wild-type *Nf2* and 442 bp band indicative of *Nf2* exon 2 flanked by LoxP sequences. Amplification with primer set P5/6 produces a 338 bp band indicative of loss of *Nf2* exon 2; B. Western blot of merlin protein expression in *Nf2^{fllox2/fllox2}* and *Nf2^{Ex2-/-}* MSCs detected with N- and C-termini antibodies; C. Crystal violet assay at 24, 48, and 48 hrs to assess cell number of merlin-null and control *Nf2^{fllox2/fllox2}* MSCs cultured in different substrates and growth media. PLL: poly-L-lysine; Lam: laminin; mitog: mitogenic factors, 10 ng/ml neuregulin and 2 μ M forskolin; D. Phase image of *Nf2^{fllox2/fllox2}* and merlin-null MSCs. Merlin-null MSCs are large and round compared to small, bipolar control SCs. E. Confocal images of *Nf2^{fllox2/fllox2}* and merlin-null MSCs at low and high density. F-actin, detected by phalloidin staining (white); S-100, SC marker (green); and DAPI, nuclear stain (blue). Scale bar: 20 μ m.

20 μ l growth medium phenol-red free and centrifuged 1 min at 500 rpm prior to incubation at

37°C, 7% CO₂ for 4-5 hours to allow attachment. Next, cultures were treated with increas-

PI3K as a pharmacological target in NF2

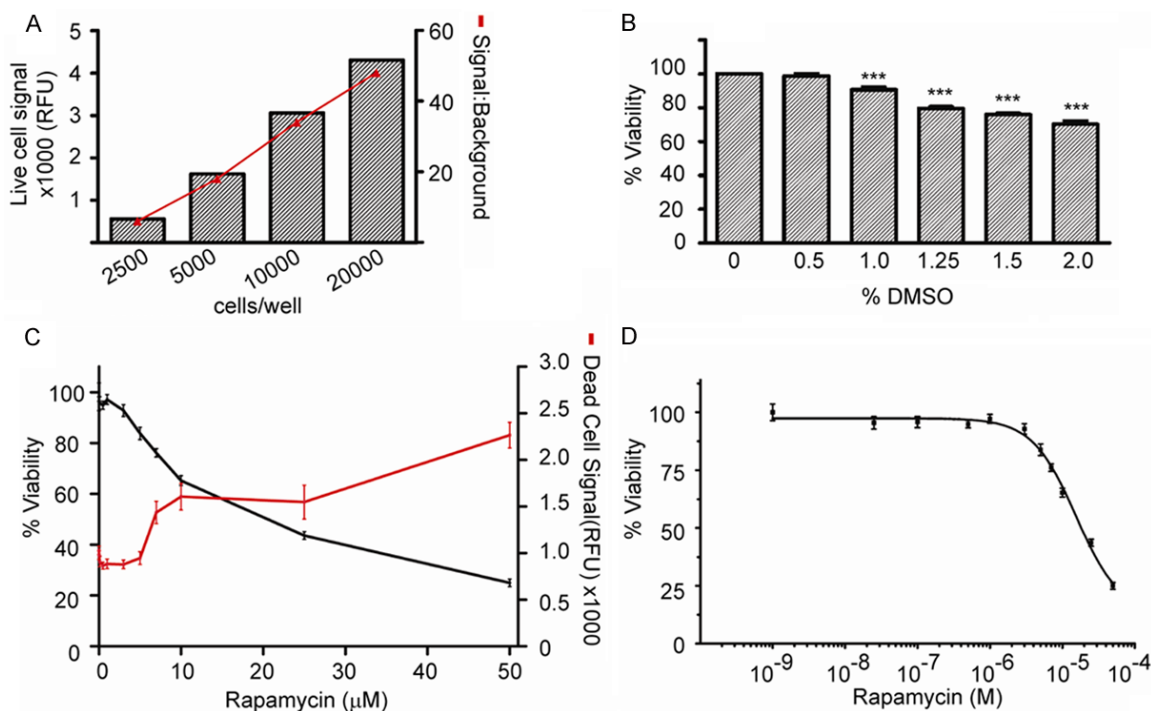


Figure 2. Optimization of Merlin-null Mouse Schwann Cell Culture Conditions for HTS and Assay Validation. A. Viability signal of merlin-null SCs at increasing seeding densities. Signal:background ratio is shown in red. Fluorescence (Ex405 nm/Em492 nm) for live cells was read 30 minutes later. Cell viability expressed as RFU (relative fluorescent units); B. DMSO tolerance. Cell viability signal expressed as percent viability with respect to control (0% DMSO). One-way ANOVA with Dunnett's *post hoc* test compared to 0% DMSO; C. Merlin-null MSC viability and cytotoxicity screen of increasing concentrations of rapamycin conducted with the MultiTox-Fluor assay. Live-cell protease signal (Ex405 nm/Em492 nm) is expressed as % viability of the DMSO control (left y-axis) and dead-cell protease signal (Ex485 nm/Em535 nm) is expressed in RFUs (right y-axis); D. Rapamycin dose response 24-hr viability analyzed by log [inhibitor] vs. viability response, non-linear regression (four parameters).

ing concentrations of AS605240 at 0.4% DMSO and staurosporine (as a positive control). Plates were spun 1 min at 500 rpm and incubated for 8 hours. Caspase 3/7 activity was assessed with the Apo-ONE homogeneous assay (Promega) following manufacturer's instructions. Fluorescence was read in a Synergy H1 Hybrid plate reader (BioTek, Winooski, VT, USA).

Membrane asymmetry assay

Merlin-null MSCs were seeded in 6-well Corning CellBIND plates at 500,000 cells per well. The next day, cells were treated for 3-5 hours with 0.1% DMSO, 0.5 μM staurosporine, and 1, 3, and 10 μM AS605240 in 0.1% DMSO in the presence or absence of the pan-caspase inhibitor Z-VAD-FMK (50 μM). After incubation, cultures were harvested and analyzed with the Violet Ratiometric Membrane Asymmetry Probe/Dead Cell Apoptosis assay (Invitrogen, Life Sciences) following manufacturer's instructions on a BD Canto-II (Becton, Dickinson and

Co, Franklin Lakes, NJ, USA) flow cytometer equipped with BD FACSDiva™ 6.1.3 software.

Autophagy assessment

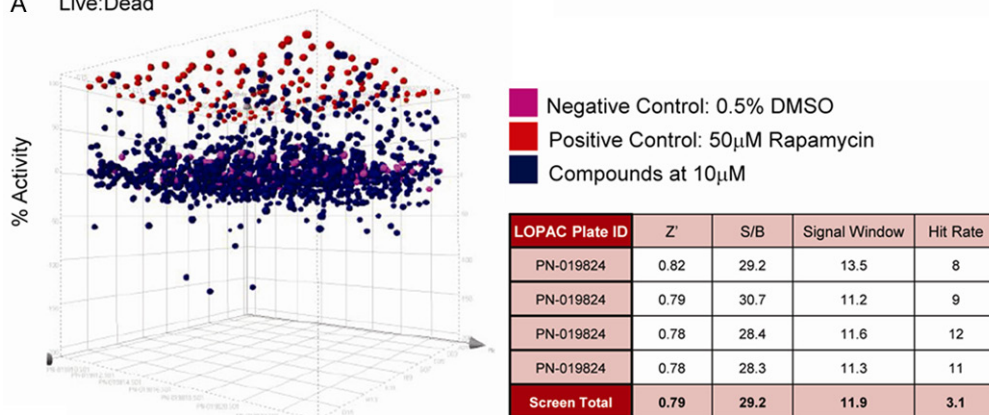
Merlin-null MSCs were seeded at 150,000 cells/well into 12-well Corning CellBIND plates. The next day, cultures were treated for 3 hrs with increasing concentrations of AS605240 in 0.02% DMSO in duplicate with and without 10 μg/ml acidic lysosomal inhibitors (E64-d and pepstatin-A). Whole-cell lysate preparation and western blots were performed as described above.

High-content image analysis

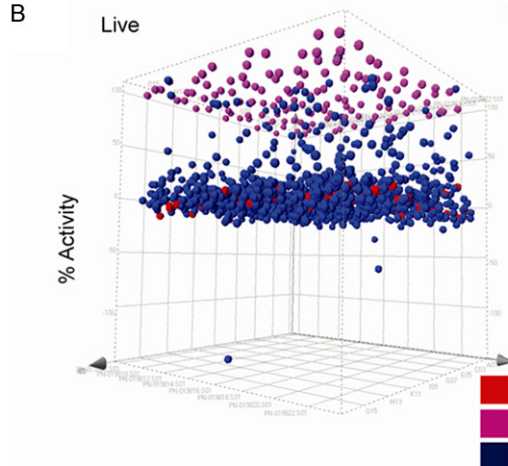
Merlin-null MSCs (1,500 cells/well) were seeded on 384-well Corning CellBIND plates and incubated at 37°C, 7% CO₂ for 4 hrs to allow complete cell attachment. Cells were treated in triplicates with increasing concentrations of

PI3K as a pharmacological target in NF2

A Live:Dead



B Live



C Dead

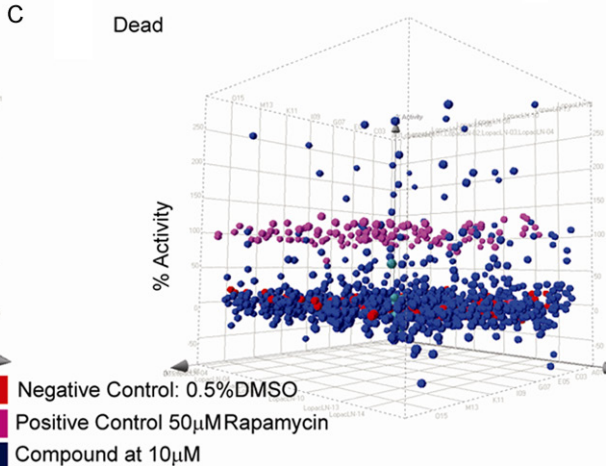


Plate ID	p1	p2	p3	p4
Pos Control	97499 + 3326	107170 + 4766	105875 + 10896	107279 + 12922
Neg Control	1180094 + 56815	1370671 + 46945	1321835 + 71952	1445531 + 61077
Signal/Background	12.1	12.8	12.5	13.5
Z Factor	0.833	0.877	0.796	0.834
Signal Window	15.9	23.6	13.4	18.3
# Hits >=50% inhib	12	12	13	35

Plate ID	p1	p2	p3	p4
Pos Control	9052825 + 510104	10445380 + 679235	10339935 + 529776	107279 + 12922
Neg Control	3761926 + 340937	4371216 + 370370	4328255 + 426091	1445531 + 61077
Signal/Background	2.41	2.39	2.31	2.2
Z Factor	0.517	0.482	0.523	0.400
Signal Window	5.37	4.31	5.93	3.14
# Hits >=50% inhib	16	15	18	22

Figure 3. 3-D Scatter Plot of LOPAC Results Using Merlin-null MSCs. A. Data represent the percent activity (Live/Dead signal; z-axis) relative to control wells by compound used in indicated locations (well position, x-axis; plate number, y-axis). LOPAC compounds (blue), negative DMSO control (0% activity, pink), and positive controls (100% activity, red symbols) at the top of the plot with putative hits. Table shows the statistics per plate and complete screen; B. Data represent the percent activity (Live signal; z-axis) relative to control wells by compound used in indicated locations (well position, x-axis; plate number, y-axis). LOPAC compounds (blue), negative DMSO control (0% activity, red), and positive controls (100% activity, pink symbols). Table shows the statistics for each plate and complete screen; C. Results for dead-cell Protease activity (Dead signal; z-axis) expressed as in B.

compounds (3 nM-10 µM in 0.5% DMSO) for 48 hrs with a brief (30 min) incubation with 10 µM EdU. Cultures were fixed with paraformaldehyde and immunostained for phospho-Histone 3 and EdU and DNA was stained with Hoechst. Wells were imaged using an automated microscope (Image Express) and analyzed with Definiens automated image analysis software to evaluate several nuclear morphometry

parameters (size, shape, and label intensities) to extract multiple classifications of cells, including S and M phases.

Statistical analysis

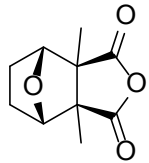
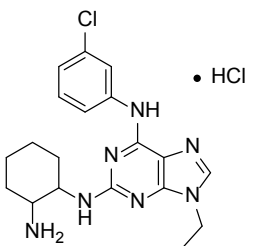
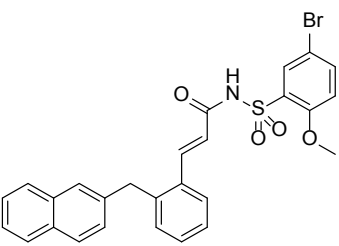
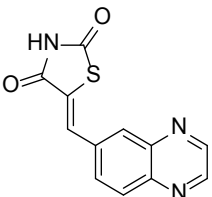
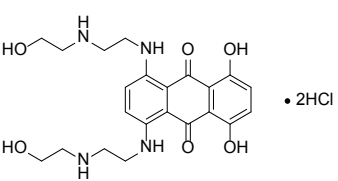
Statistical analysis and graph generation was performed with GraphPad Prism version 5.0 for Windows (GraphPad, La Jolla, CA, USA). Dose-

PI3K as a pharmacological target in NF2

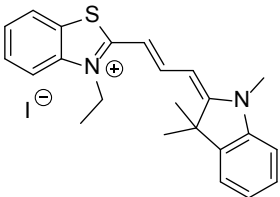
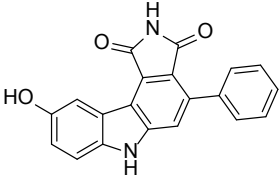
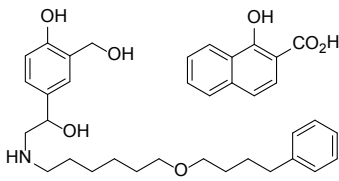
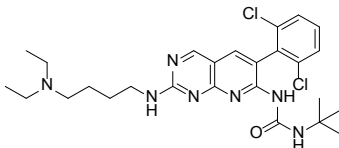
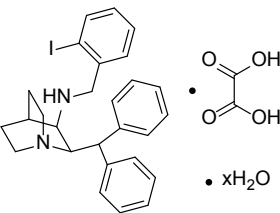
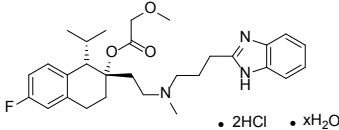
Table 1. Summary of Confirmation and Selectivity Assays

Compound ID	Compound Structure	Primary Assay (% Viability)	Orthogonal Assay (% Viability)	Selectivity Assay (% Viability)	Fold Selectivity at 10 μ M	Description
L663536 (MK-886)		16 \pm 3	0.1	31	1.9	Potent, specific leukotriene biosynthesis inhibitor
Ebastine		17 \pm 3	0.1	31	1.8	Non-sedating histamine H1 receptor antagonist
BNTX maleate salt hydrate		19 \pm 4	35.3	32	17	Selective δ 1 non-peptide opioid receptor antagonist
GW7647		20 \pm 5	6.3	32	1.6	Potent human PPAR α agonist
BIO		20 \pm 8	0.8	31	1.5	Potent, reversible ATP-competitive GSK-3 α / β inhibitor
GW5074		24 \pm 7	36.4	31	1.3	cRaf1 kinase inhibitor

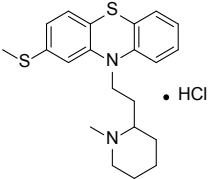
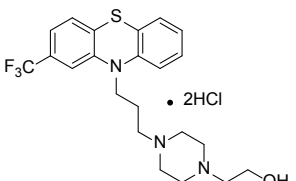
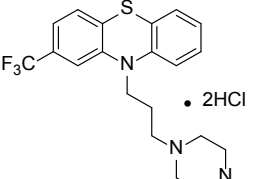
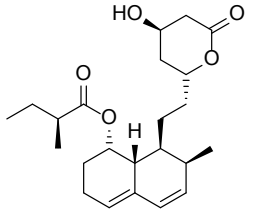
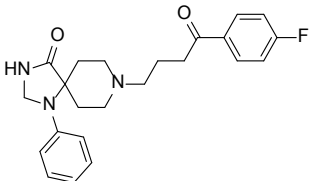
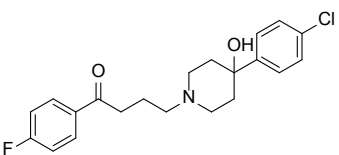
PI3K as a pharmacological target in NF2

Cantharidin		34 ± 14	35.2	78	2.3	Protein phosphatase1 (PP1) and PP2A inhibitor
CGP-74514A hydrochloride		35 ± 7	16.1	33	0.9	Cyclin-dependent kinase inhibitor selective for Cdk-1
L-798106		35 ± 13	37.6	33	0.9	EP3-selective antagonists
AS605240		35 ± 2	40.1	78	2.2	Potent, selective PI3Kγ inhibitor
Mitoxantrone dihydrochloride		39 ± 6	36.8	34	0.9	DNA intercalator, increases double-strand breaks, stabilizes topoisomerase II

PI3K as a pharmacological target in NF2

AC-93253 iodide		41 ± 6	24.3	28	0.7	Cell permeable, subtype selective RAR (RAR α) agonist
PD-407824		43 ± 10	34.5	37	0.9	Wee/Chk1 inhibitor
Salmeterol xinafoate		57 ± 9	73.7	57	1	β 2-adrenoceptor agonist
PD-161570		60 ± 12	62.4	47	0.8	Human FGF-1 receptor tyrosine kinase inhibitor
L-703606 oxalate salt hydrate		62 ± 11	40.6	33	0.5	Potent, selective non-peptide NK-1 tachykinin receptor antagonist
Mibefradil dihydrochloride hydrate		67 ± 9	53.3	32	0.5	T-type Ca ²⁺ channel blocker; anti-hypertensive

PI3K as a pharmacological target in NF2

Thioridazine hydrochloride		71 ± 13	67.9	33	0.5	D ₂ dopamine receptor antagonist
Fluphenazine dihydrochloride		71 ± 6	45.6	43	0.6	D ₁ /D ₂ dopamine receptor antagonist, H ₁ histamine receptor antagonist
Trifluoperazine dihydrochloride		78 ± 6	47	47	0.6	D ₂ dopamine receptor antagonist, inhibits calmodulin-dependent stimulation of 3':5'-cyclic nucleotide phosphodiesterase, inhibits cAMP-gated cation channels
Mevastatin		81 ± 11	85.1	74	0.9	HMG-CoA reductase inhibitor
Spiroperidol		90 ± 6	84.3	85	1.1	Selective D ₂ dopamine receptor antagonist, α _{1B} -adrenoceptor antagonist, mixed 5-HT _{2A} /5-HT ₁ serotonin receptor antagonist
Haloperidol		96 ± 4	88.8	78	0.8	Dopamine antagonist with selectivity for D ₂ -like receptors

response experiments were analyzed by non-linear regression (four parameters). Experimental data were statistically analyzed as indicated for each experiment.

Results

Creation and characterization of merlin-null mouse schwann cells

A merlin-null MSC line was created by isolating SCs from homozygous *Nf2^{fllox2/fllox2}* mice. These mice have two *loxP* sequences flanking exon 2 of the *Nf2* gene. Cells were transduced with adeno-Cre to delete exon 2. The homozygous insertion of the *loxP* sequences and deletion of *Nf2* exon 2 was verified by PCR analysis of genomic DNA (**Figure 1A**). The first PCR with primers P4/P5 amplified a 305 bp band for wild-type *Nf2* FVB/N mice, two bands at 305 bp and 442 bp for heterozygous *Nf2^{fllox2/+}* mice, and a single 442 bp band for *Nf2^{fllox2/fllox2}* mice. The second PCR with primers P6/P5 amplified a single 338 bp band for two independent cell derivations of merlin-null MSCs used in our experiments, confirming the loss of exon 2 in the *Nf2* gene (**Figure 1A**). Western blot analysis with an antibody for the N-terminus of merlin showed the merlin band present in *Nf2^{fllox2/fllox2}* MSCs, but not in merlin-null MSCs. Western blot analysis with an antibody raised against a C-terminal merlin peptide revealed that merlin is expressed at lower levels in merlin-null MSCs than in *Nf2^{fllox2/fllox2}* MSCs, which is in agreement with the rapid degradation of mutant versus wild-type merlin protein (**Figure 1B**). To assess the growth rate of control and merlin-null MSCs and their dependence on substrates and mitogenic factors, we measured the number of viable cells at various time points. Control MSCs grew slowly and only on a poly-L-lysine and laminin substrates in serum-free medium supplemented with forskolin and neuregulin. By contrast, merlin-null MSCs grew on uncoated plastic in serum-free medium lacking the mitogenic supplements forskolin and neuregulin (**Figure 1C**). These data suggest that loss of functional merlin allows SCs to grow independently of mitogenic factors and extracellular matrix substrates. Merlin-null MSCs also lost the typical bipolar morphology characteristic of wild-type SCs (**Figure 1D**). In addition, unlike primary mouse SCs that senesce after 3-4 passages, merlin-null MSCs became immortalized and failed to arrest at high density (**Figure 1E**). We also showed by immunostaining that merlin-

null MSCs retained expression of the SC marker S-100 (**Figure 1E**). In summary, the cells described here are functionally merlin-null MSCs that replicate the morphological phenotype of human schwannoma cells.

Optimization and validation of merlin-null MSCs for HTS assays

To determine whether the generated cell line was amenable to a HTS platform, we tested cell adherence and growth after 24 hrs of incubation on 384-well plates from different manufacturers at multiple cell densities (2,500-20,000 cells/well) (**Supplementary Figure S1A-D**). Merlin-null MSCs attached well and formed a monolayer on plates coated with PLL and on Corning CellBIND plates. To select the optimal seeding density for the assay, we treated half of the wells with 27 µg/ml digitonin and measured the ratio of live to dead cells using the MultiTox-Fluor Multiplex Cytotoxicity Assay. The signal to noise ratio, signal to background ratio, and Z' factor were also calculated [24] (**Supplementary Figure S1A-D**). We selected the Corning CellBIND plates seeded at 5,000 cells/well for the screening assay [25] (**Figure 2A** red-lined graph). We tested DMSO tolerance of the merlin-null MSCs and found a 10% loss of cell viability at the 1% DMSO concentration typically used in compound screens (**Figure 2B**). Therefore, the DMSO concentration for screening was maintained at 0.5%. To confirm the viability assay in a 384-well plate format with merlin-null MSCs, we treated the cells with increasing concentrations of rapamycin, an mTOR (mammalian target of rapamycin) inhibitor known to reduce proliferation of cells lacking merlin function [26, 27]. We measured live-cell protease signal (expressed as % of DMSO control) and dead-cell protease signal (expressed as relative fluorescence intensity) 24 hrs later (**Figure 2C**). Viability of cells treated for 24 hrs with 50 µM rapamycin was 20±1.4% of the DMSO control. We selected 50 µM rapamycin as our positive control for statistical/quality control analysis of assay performance in the compound screen. Repetitions of the dose-response experiments using the live-cell protease assay provided a consistent IC₅₀ of 15 µM for 24 hrs incubation (**Figure 2D**).

LOPAC screen with merlin-null mouse Schwann cells

We performed a screen of the LOPAC (Sigma's LOPAC^{®1280} library). We tested merlin-null MSC

PI3K as a pharmacological target in NF2

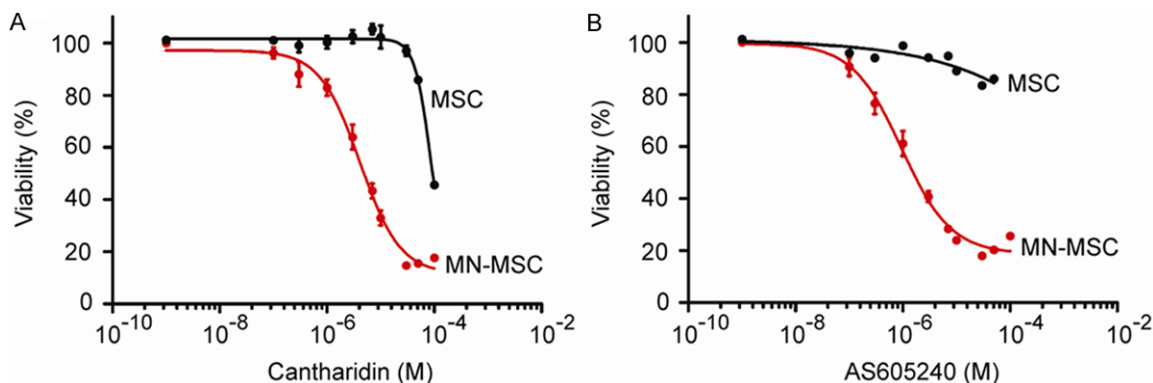


Figure 4. Dose-Response Plots of AS605240 and Cantharidin in Merlin-null and Control MSCs. Viability dose-response study performed in a 384-well format for cantharidin (A) and AS605240 (B). Cell viability was measured with the live-cell protease assay after 24 hrs incubation with the compounds. Graph represents the mean \pm SEM of 2 independent experiments with 8 replicates for each concentration analyzed together ($n=16$). MSC, control MSC ($n=8$). Dose response analyzed as log [inhibitor] vs. viability response, non-linear regression (four parameters).

viability after 24 hr incubation with the compounds at 10 μ M in 0.5% DMSO in single wells. Each of the four assay plates had positive and negative controls, cells treated with 50 μ M rapamycin in 0.5% DMSO and cells treated with 0.5% DMSO alone. The screening assay (live: dead cell ratio) had a Z' value of 0.79 and yielded 40 hits (3.1%) using a cut-off value equal to 80% of the live: dead signal of the DMSO negative control (**Figure 3A**). The MultiTox-Fluor Multiplex Cytotoxicity Assay, a dual viability and cytotoxicity assay, proved to be highly sensitive based on the live: dead ratio for cultures treated with compounds at 10 μ M. Therefore, we assessed the quality of the live and dead readouts separately. The plate statistics of the four plates were consistent, with a Z' \sim 0.8 for the viability assay. Signal confidence for the dead-cell protease was weaker with a Z' \leq 0.5. The hit rate was equivalent to a cut-off value of 50% of live-cell signal alone (< 50% viability) (**Figure 3B, 3C**). Complete library screen hit data is shown in [Supplementary Figure S2](#).

Compound confirmation and selectivity assays

We selected 20 hit compounds for confirmation studies based on target specificity and potential therapeutic value. We also included three compounds that had higher target specificity and/or affinity than its LOPAC hit. Two dopamine receptor D₂ antagonists were hits. One, trifluoperazine dihydrochloride, is also a weak antagonist of the 5HT-2 serotonin receptor, inhibits calmodulin-dependent stimulation of 3': 5'-cyclic nucleotide phosphodiesterase, and inhibits cAMP-gated cation channels. No other

compounds targeting Nav1.7 and Nav1.4 present in the library were hits. The other, thioridazine hydrochloride, also antagonizes Ca²⁺ channels. Therefore, for the confirmatory screens, we added three more selective D₂ antagonists: fluphenazine dihydrochloride, spiperone, and haloperidol.

For the confirmation assays, all compounds were tested under the same conditions, 24 hr incubation at 10 μ M in 384-well Corning CellBIND plates using the live-cell protease assay (CellTiter-Fluor). We repeated the assays four times on two independently-derived merlin-null MSC lines, L10, the same one used in the LOPAC screen, at passages 13 and 23, and L08, tested at passages 20 and 21 (**Table 1**, Primary assay). To corroborate the fluorogenic CellTiter viability results, we measured cell viability with an orthogonal assay that assesses ATP levels using a thermostable luciferase to generate a luminescent signal (CellTiter-GLO, Promega) (**Table 1**, Orthogonal assay). To identify compounds/targets with potential therapeutic value, we tested the effect of the compounds on control *Nf2*^{fllox2/fllox2} MSCs. The selectivity assay was conducted using control cells at passage 2 in 8 replicates with the primary fluorescence viability assay. The results of this counter-screen are shown in **Table 1**.

In summary, we confirmed the majority of the LOPAC hits with both primary and orthogonal assays (> 50% loss of merlin-null MSC viability compared to DMSO control) and identified only two compounds that demonstrated selectivity for merlin-null versus wild-type MSCs.

PI3K as a pharmacological target in NF2

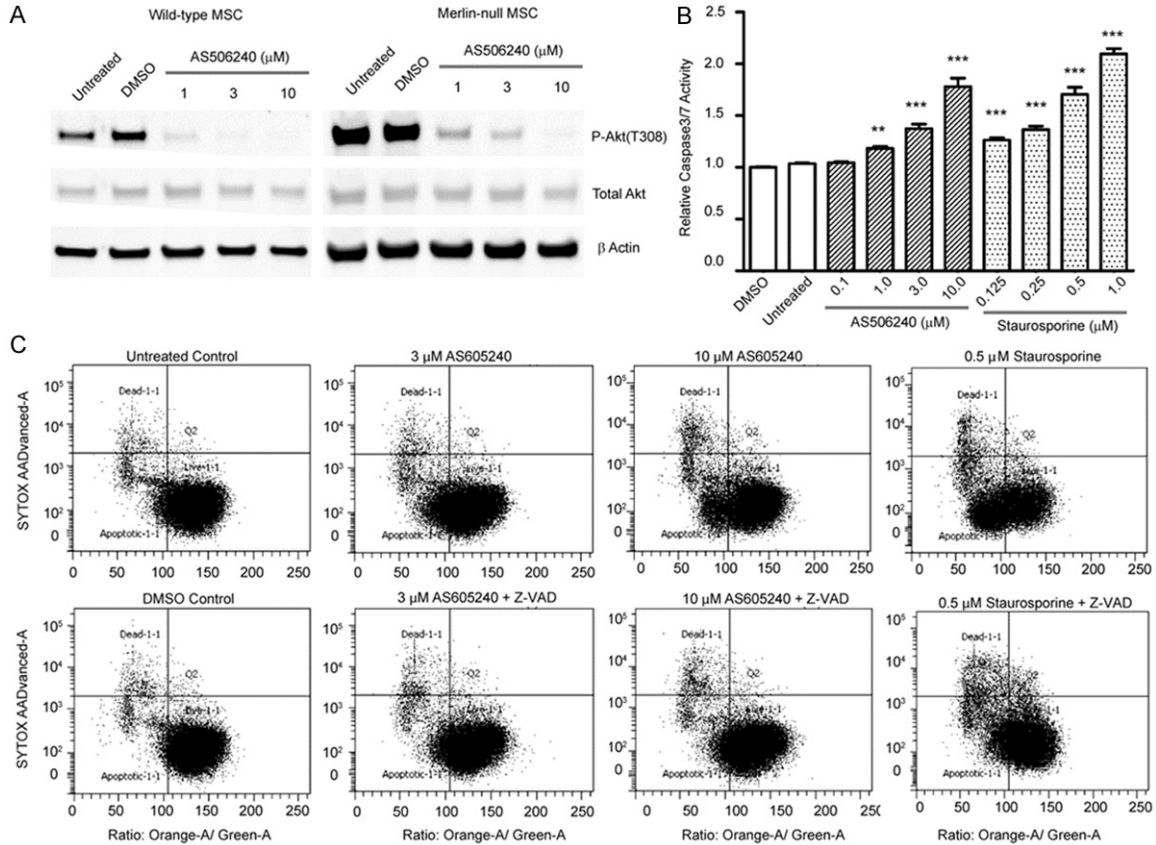


Figure 5. AS605240 Induces Caspase-Dependent Apoptosis in a Dose-Dependent Manner. A. AS605240 effectively decreased phosphorylation of Akt in a dose-dependent manner. Western blot of control and merlin-null MSCs treated with increasing concentrations of AS605240 for 6 hrs. Membrane was blotted with antibodies against phosphor-Akt, Akt, and β -actin (as a loading control); B. Caspase 3/7 activity assay. Merlin-null MSCs were treated for 8 hrs with increasing concentrations of AS605240 and caspase 3/7 activity was measured with a plate fluorescence assay. Graph represents mean \pm SEM of three independent experiments. One-way ANOVA, Bonferroni's post test compared to DMSO control. ** $p < 0.01$ and *** $p < 0.001$; C. Representative membrane asymmetry assay of merlin-null MSCs treated with increasing concentrations of AS605240 in the presence and absence of the pan-caspase inhibitor Z-VAD-FMK (50 μ M). After 4 hrs incubation, the samples were analyzed by flow cytometry to quantify the live-, apoptotic-, and dead-cell populations.

PI3K inhibitor AS605240 and PP1/ PP2A inhibitor cantharidin selectively decrease merlin-null mouse Schwann cell viability in a dose-dependent manner

AS605240, a selective PI3K γ inhibitor, and cantharidin, an inhibitor of protein phosphatase 1 and 2A (PP1 and PP2A), were highly selective for merlin-null MSCs. Both caused \sim 65% loss of viability of merlin-null MSCs and $<$ 22% loss of viability of control MSCs. We conducted dose-response experiments for AS605240 and cantharidin on merlin-null and control MSCs. Cells were incubated for 24 hrs with increasing concentrations of AS605240 or cantharidin and viability was assessed using the CellTiter-Fluor assay. Cantharidin had an IC_{50} = 4.1 μ M for

merlin-null MSCs and an IC_{50} = 85.4 μ M for control cells (Figure 4A). The PI3K inhibitor AS605240 decreased viability of merlin-null MSCs in 24 hrs with an IC_{50} = 0.95 μ M, whereas the IC_{50} for the control MSCs could not be calculated because the drug did not significantly reduce viability at any of the tested concentrations (Figure 4B). These results suggest that both compounds are highly selective for merlin-null MSCs in a dose-dependent manner.

AS605240 induces merlin-null mouse Schwann cell caspase-dependent apoptosis and autophagy

Because AS605240 exhibited lower IC_{50} values and greater selectivity for merlin-null MSCs

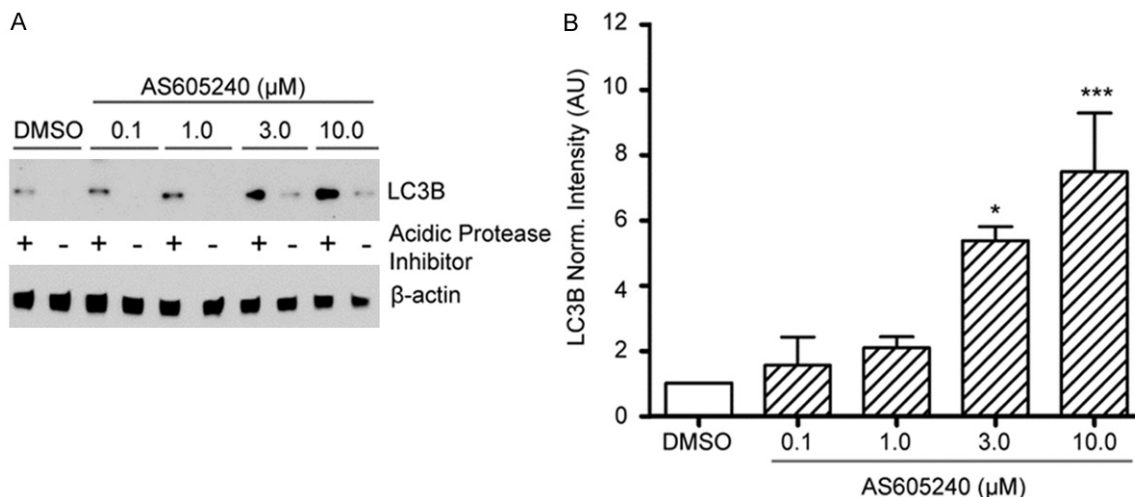


Figure 6. AS605240 Induces Autophagy in a Dose-Dependent Manner. A. Western blot for anti-LC3B of merlin-null MSCs treated with increasing concentrations of AS605240 in the presence and absence of lysosomal protease inhibitors (10 μg/ml E64-d and pepstatin-A). Anti-β-actin was used as a loading control; B. Quantitation of LC3B western blot by densitometry analysis. *p < 0.05; ***p < 0.001 by one-way ANOVA, Bonferroni's post test (n=4).

than cantharidin, we selected AS605240 for further phenotypic studies to determine how it reduces cell viability. First, we verified AS605240 activity on its target in merlin-null MSCs by western blotting with an antibody against the phosphorylated form of Akt as a downstream indicator of PI3K activity. After 6 hrs incubation, AS605240 decreased Akt phosphorylation levels in a dose-dependent manner (**Figure 5A**). To evaluate if AS605240 selectively decreased viability of merlin-null MSCs via apoptosis, we measured caspase 3/7 activity using a plate fluorescence assay. Serial dilutions of staurosporine were used as a positive control. AS605240 treatment induced caspase 3/7 activity in merlin-null MSCs in a dose-dependent manner (**Figure 5B**). To determine if the apoptotic pathway was only caspase-dependent, we performed a membrane asymmetry assay by flow cytometry in the presence and absence of a pan-caspase inhibitor. The percentage of cells undergoing apoptosis (caspase-dependent or -independent) in cultures treated with DMSO was 4.3±0.8%. By contrast, when cultures were treated with 3 and 10 μM AS605240, apoptosis levels increased to 9.3±1.5% and 12.5±1.4%, respectively. When cultures were treated simultaneously with AS605240 and a general caspase inhibitor Z-VAD-FMK (peptide sequence Z-Val-Ala-Asp-CH₂F), the apoptotic levels returned to 5%, similar to DMSO control levels, suggesting induction of a caspase-dependent apoptosis pathway (**Figure 5C**).

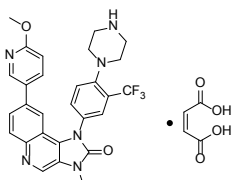
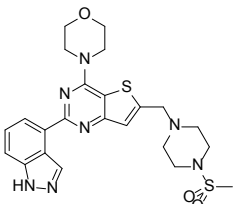
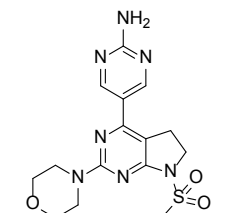
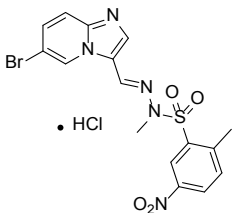
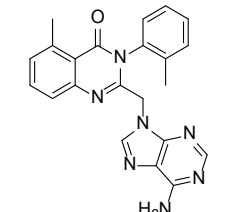
We also investigated the ability of AS605240 to induce cell autophagy. We used microtubule-associated protein 1A/1B light chain protein 3 conversion (LC3B-II) as a marker of autophagy [28]. Merlin-null MSCs were treated with increasing concentrations of AS605240 for 3 hrs, with and without the lysosomal protease inhibitors E64d and Pepstatin A to preserve a readout for autophagy that can be lost in cells with accelerated lysosomal flow. Western blot for LC3B-II showed that AS605240 induced autophagy in a dose-dependent manner (**Figure 6A, 6B**). The results indicate that AS605240 reduced merlin-null MSC viability via caspase-dependent apoptosis accompanied by significant induction of autophagy.

Additional testing of PI3K inhibitors currently in clinical trials

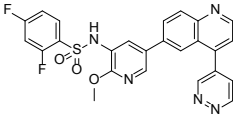
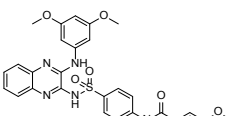
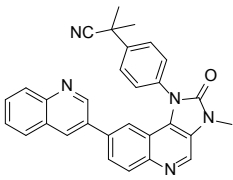
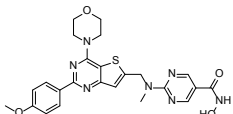
Because PI3K showed potential as a target for NF2 therapy, we used a high-content screening (HCS) approach to test PI3K inhibitors currently in clinical trials for cancer. The HCS approach also allowed us to begin building multi-parametric phenotypic signatures for each treatment tested, thereby establishing a stronger basis for more accurate comparative analyses. Merlin-null MSCs were seeded in 384-well Corning CellBIND plates and incubated for 48 hrs after attachment with increasing concentrations of the drugs. Cells were briefly incubated with EdU prior to fixation and prepared for

PI3K as a pharmacological target in NF2

Table 2. Summary of Activity of Various PI3K Inhibitors.

Compound ID	Structure	Target	Viability IC ₅₀ (μM)	Number of nuclei	DNA replication index	Mitotic index	Large nuclei	Small nuclei	Condense nuclei
NVP-BGT226		PI3Kα/γ/β	0.06	↓↓↓	↓↓↓	↓↓↓	↓↓↓	↑↑↑	↓↓
GDC-0941		PI3Kα/δ	0.02	↓↓↓	↓↓↓	↓↓	↓	↑	↑↑
CH-5132799		PI3Kα	0.98	↓↓	↓↓	-	↑	-	-
PIK-75		PI3Kα	0.02	↓↓↓	↓↓↓	↑	↑↑↑	↑↑↑	↑
IC-87114		PI3Kδ	-	-	-	-	-	-	-

PI3K as a pharmacological target in NF2

GSK-2126458		PI3K/ mTOR	0.02	↓↓↓	↓↓↓	↑	↑↑↑	↑↑↑	↑
XL-765		PI3K γ / mTOR	2.16	↓↓	↓↓	↑	-	-	-
BEZ-235		PI3K/ mTOR	0.1	↓↓↓	↓↓↓	↓↓↓	↓↓↓	↑	↑↑↑
CUDC-907		PI3K/ HDAC	0.03	↓↓↓	↓↓↓	↑	↑↑↑	↑↑↑	↑

↓↓↓ strong decrease, ↓↓ moderate decrease, ↓ weak decrease, ↑↑↑ strong increase, ↑↑ moderate increase, ↑ weak increase, - no change.

multi-parametric automated microscopy and image analysis. Several readouts were selected to document cytostatic and cytotoxic effects, while also providing insight into underlying cellular mechanisms with respect to cell cycle progression, apoptosis, and necrosis. Thus, EdU incorporation provided an index of S-phase cells, phosphoSer10-Histone 3 immunostaining provided an index of M-phase cells (mitotic index), and Hoechst staining enabled nuclear morphometric analysis based on nuclear size, shape, and condensation. Combined with the other readouts, nuclear morphometry signatures were used to document more accurately a variety of specific phenotypes, such as G2 arrest with large nuclei, apoptotic cells with highly condensed nuclei, and dying cells with small nuclei. Of the 9 compounds tested, 5 targeted PI3K alone: PIK-75, CH-5132799, IC-87114, BGT226, and GDC0941. BEZ235, XL-765, and GSK-2126458 are dual inhibitors of PI3K and mTOR and CUDC 907 inhibits PI3K and histone deacetylase (HDAC) 1/2/3/10. Results are summarized in **Table 2**. All compounds but one effectively decreased viability of merlin-null MSCs causing a strong decrease in the mitotic index and an increase in the number of dying cells. The exception was IC-87114 which selectively inhibits PI3K δ over the other isoforms (*in vitro* kinase assay PI3K δ IC_{50} = 0.5 μ M compared to 75 μ M and 29 μ M for PI3K β and γ , respectively) [29]. The compounds had strong anti-proliferative effects, causing cell death through apoptotic mechanisms with varying kinetics. The dual inhibitors additionally caused cell cycle arrest of merlin-null MSCs. Taken together, the results strongly suggest that PI3K is a candidate NF2 drug target.

Discussion

LOPAC screen using a phenotypic viability assay

Because there is a great need for chemotherapeutic options for NF2, we developed an NF2 cellular model and performed a proof-of-concept phenotypic HTS of the LOPAC. The LOPAC screen identified various compounds that decreased merlin-null MSC viability. Among them were pro-apoptotic agents, inhibitors of signaling kinases, cell-cycle inhibitors, receptor inhibitors, and modulators of cell metabolism (**Supplementary Figure 2**). One of the identified compounds, the sirtuin 2 inhibitor AGK2, was independently studied and validated [30].

Approximately half of the compounds modulated components in the known merlin-dependent pathways; however, all but two compounds reduced the viability of normal MSCs equally. Our funneling confirmatory and counter-screens identified two selective compounds, cantharidin and AS605240. In fact, cantharidic acid and cantharidin were both hits in the LOPAC screen, but because cantharidic acid has been reported to produce serious liver toxicity, only cantharidin was included in our confirmatory screens [31].

PI3K identified as potential target for NF2 therapeutics

Because merlin inhibits the PI3K/Akt pathway and loss of merlin activates PI3K in cells, targeting PI3K would seem to hold therapeutic potential for NF2 [11, 13]. AS605240 is an ATP-competitive PI3K inhibitor with differential isoform selectivity. According to the *in vitro* kinase assay the IC_{50} of isoform γ is 8 nM, α is 60 nM, β is 270 nM, and δ is 300 nM [32]. This compound decreased merlin-null MSC viability in a potent and selective fashion, with an IC_{50} = 0.95 μ M. Interestingly, derivatives of AS605240 have been reported to interfere with glioma cell proliferation *in vitro* [33]. Similar to our finding that AS605240 inhibits merlin-null MSCs via an apoptotic mechanism, AS605240 induced apoptosis of PI3K γ -positive neuroblastoma cells [34]. Supporting and further characterizing the inhibitory mechanism of AS605240 against the PI3K/Akt pathway, recent reports suggest that activated Akt affects the apoptosis pathway directly by targeting and down-regulating the pro-apoptotic activity of BAD and BAX, Bcl-2 family members, resulting in cell survival [14]. In addition, the PI3K/Akt pathway modulates cell death and survival through NF- κ B regulation of pro- and anti-apoptotic genes [35]. Moreover, loss of merlin activity leads to accumulation of activated ErbB2/3 receptors at the plasma membrane of SCs, *Nf2* mutant mouse peripheral nerves, and human NF2 schwannomas, whereas the reintroduction of merlin decreases their levels in primary SCs [36]. Activation of the heterodimeric ErbB2/3 receptor in primary SCs activates PI3K and inhibition induces apoptosis by blocking Akt and Bad phosphorylation [37]. To capitalize on PI3K as a potential therapeutic target for NF2, we tested, in addition to AS605240, the potency of other small molecule PI3K inhibitors with different chemical structures. Similar to the strong

antitumor activity exhibited by CH5132799, PIK75, and GDC0941 in various cancer cell lines (e.g., human 2008, SK-OV-3, IGROV1, COLO-704, and OVCAR-3), breast cancer cell lines (e.g., KPL-4, BT-483, T-47D, MDA-MB-453, MDA-MB-361, JMT-1, HCC1954, and HCC-1599), human prostate cancer cell lines (e.g., PC-3, 22Rv1, LNCaP-CS10, and LNCaP-BC2, DU145), and endothelial cancer cell lines (e.g., HEC1B, AN3-CA, MFE-280, MEF-296, and HEC-1-A), we found that these compounds had strong anti-proliferative activity against merlin-null MSCs [38-41]. As with all kinase inhibitors, the compounds we tested may act at more than one kinase target; however, the calculus of the various structures, their collective effect on merlin-null MSCs, and common pharmacology (PI3K inhibition) all support further validation and characterization of the role of PI3K in merlin tumor suppression and NF2 pathogenesis.

Combined target inhibition

Several PI3K inhibitors are currently in clinical trials for treatment of various cancers. Among these are pan-PI3K, PI3K isoform-selective inhibitors and dual PI3K/ mTOR inhibitors that have exhibited encouraging safety, efficacy, pharmacokinetic, and pharmacodynamic profiles. The heterogeneity and adaptive nature of tumors often limit the therapeutic success of single-target compounds because of concurrent activation of other signaling pathways that facilitate tumor survival and proliferation. Thus, we tested four dual-target compounds currently in clinical trials. One class of compounds tested has combined PI3K and mTOR inhibitory activity. Inhibition of mTOR alone with rapamycin resulted in Akt activation caused by loss of the p71 S6K1 negative feedback loop in patients [42]. Thus, small molecules that inhibit two components of the pathway simultaneously were developed [43, 44]. We found that BEZ-235, XL-765, and GSK-2126458 exerted strong anti-proliferative effects (very low IC_{50}) in merlin-null MSCs by blocking cell cycle progression (G1 arrest and possibly also G2 arrest for GSK-2126458) and stimulating cell death, in contrast to the predominant apoptotic action of PI3K single-target inhibitors. In agreement with our findings, BEZ-235 and GSK-2126458 have been reported to induce cell cycle arrest, particularly at G1, rather than induce apoptosis in breast cancer cells [45]. The other class of compounds tested, which includes CUDC-907, has combined PI3K and HDAC inhibitory activi-

ty. We found that CUDC-907 potently decreased merlin-null MSC viability via G2 arrest and cell death ($IC_{50}=0.03 \mu\text{M}$). Similarly, CUDC-907 exhibited potent growth inhibition of diverse hematologic and solid tumor cancer cell lines [46].

In conclusion, we report the completion of a successful LOPAC HTS for NF2. The unbiased screen identified PI3K as potential NF2 therapeutic target. Significantly, PI3K-dependent pathways are deregulated after loss of merlin function. Confirmatory studies on AS605240 and a series of PI3K inhibitory compounds indicated that inhibition of PI3K can promote caspase-dependent apoptosis or inhibit proliferation of merlin-null MSCs. These results validate the HT approaches and cell line as valuable tools for NF2 drug discovery. Moreover, the results indicate that PI3K inhibitors warrant further evaluation as potential NF2 therapeutics.

Acknowledgements

We thank Dr. Marco Giovaninni for the *Nf2^{flox2/flox2}* mice, Michelle Posadas, Miranda Singleton and Ada Koo for technical assistance, and Dr. Alicja Copik and Jeremiah Oyer for assistance with violet ratiometric assays. This work was supported by grants to CFV from DHHS/NIH (5R01DC10189) and the Children's Tumor Foundation (Drug Discovery Award; Young Investigator Award to A.P.), and in part by the Florida Translational Research Program at Sanford Burnham to L.H.S. (FL DOH 11SB1).

Disclosure of conflict of interest

None.

Address correspondence to: Dr. Cristina Fernández-Valle, Burnett School of Biomedical Science, College of Medicine, University of Central Florida, 6900 Lake Nona Blvd, Orlando, FL 32827, USA. Tel: 407-226-7033; Fax: 407-266-7002; E-mail: cfv@ucf.edu

References

- [1] Baser ME; Contributors to the International NF2 Mutation Database. The distribution of constitutional and somatic mutations in the neurofibromatosis 2 gene. *Hum Mutat* 2006; 27: 297-306.
- [2] Rouleau GA, Merel P, Lutchman M, Sanson M, Zucman J, Marineau C, Hoang-Xuan K, Demczuk S, Desmaze C, Plougastel B, et al. Alteration in a new gene encoding a putative

- membrane-organizing protein causes neurofibromatosis type 2. *Nature* 1993; 363: 515-521.
- [3] Trofatter JA, MacCollin MM, Rutter JL, Murrell JR, Duyao MP, Parry DM, Eldridge R, Kley N, Menon AG, Pulaski K, et al. A novel moesin-, ezrin-, radixin-like gene is a candidate for the neurofibromatosis 2 tumor suppressor. *Cell* 1993; 75: 826.
- [4] Evans DG. Neurofibromatosis type 2 (NF2): a clinical and molecular review. *Orphanet J Rare Dis* 2009; 4: 16.
- [5] Tsukita S, Oishi K, Sato N, Sagara J, Kawai A and Tsukita S. ERM family members as molecular linkers between the cell surface glycoprotein CD44 and actin-based cytoskeletons. *J Cell Biol* 1994; 126: 391-401.
- [6] Stamenkovic I and Yu Q. Merlin, a "magic" linker between extracellular cues and intracellular signaling pathways that regulate cell motility, proliferation, and survival. *Curr Protein Pept Sci* 2010; 11: 471-484.
- [7] Giovannini M, Robanus-Maandag E, van der Valk M, Niwa-Kawakita M, Abramowski V, Goutebroze L, Woodruff JM, Berns A and Thomas G. Conditional biallelic Nf2 mutation in the mouse promotes manifestations of human neurofibromatosis type 2. *Genes Dev* 2000; 14: 1617-1630.
- [8] Gautreau A, Manent J, Fievet B, Louvard D, Giovannini M and Arpin M. Mutant products of the NF2 tumor suppressor gene are degraded by the ubiquitin-proteasome pathway. *J Biol Chem* 2002; 277: 31279-31282.
- [9] Manetti ME, Geden S, Bott M, Sparrow N, Lambert S and Fernandez-Valle C. Stability of the tumor suppressor merlin depends on its ability to bind paxillin LD3 and associate with beta1 integrin and actin at the plasma membrane. *Biol Open* 2012; 1: 949-957.
- [10] Yang C, Asthagiri AR, Iyer RR, Lu J, Xu DS, Ksendzovsky A, Brady RO, Zhuang Z and Lonser RR. Missense mutations in the NF2 gene result in the quantitative loss of merlin protein and minimally affect protein intrinsic function. *Proc Natl Acad Sci U S A* 2011; 108: 4980-4985.
- [11] Rong R, Tang X, Gutmann DH and Ye K. Neurofibromatosis 2 (NF2) tumor suppressor merlin inhibits phosphatidylinositol 3-kinase through binding to PIKE-L. *Proc Natl Acad Sci U S A* 2004; 101: 18200-18205.
- [12] Ye K, Hurt KJ, Wu FY, Fang M, Luo HR, Hong JJ, Blackshaw S, Ferris CD and Snyder SH. Pike. A nuclear gtpase that enhances PI3kinase activity and is regulated by protein 4.1N. *Cell* 2000; 103: 919-930.
- [13] Hilton DA, Ristic N and Hanemann CO. Activation of ERK, AKT and JNK signalling pathways in human schwannomas in situ. *Histopathology* 2009; 55: 744-749.
- [14] Cantley LC. The phosphoinositide 3-kinase pathway. *Science* 2002; 296: 1655-1657.
- [15] Jiang BH and Liu LZ. PI3K/PTEN signaling in angiogenesis and tumorigenesis. *Adv Cancer Res* 2009; 102: 19-65.
- [16] Stokoe D. The phosphoinositide 3-kinase pathway and cancer. *Expert Rev Mol Med* 2005; 7: 1-22.
- [17] Leever SJ, Vanhaesebroeck B and Waterfield MD. Signalling through phosphoinositide 3-kinases: the lipids take centre stage. *Curr Opin Cell Biol* 1999; 11: 219-225.
- [18] Kok K, Nock GE, Verrall EA, Mitchell MP, Hommes DW, Peppelenbosch MP and Vanhaesebroeck B. Regulation of p110delta PI 3-kinase gene expression. *PLoS One* 2009; 4: e5145.
- [19] Metjian A, Roll RL, Ma AD and Abrams CS. Agonists cause nuclear translocation of phosphatidylinositol 3-kinase gamma. A Gbeta-gamma-dependent pathway that requires the p110gamma amino terminus. *J Biol Chem* 1999; 274: 27943-27947.
- [20] Wymann MP and Pirola L. Structure and function of phosphoinositide 3-kinases. *Biochim Biophys Acta* 1998; 1436: 127-150.
- [21] Akinleye A, Avvaru P, Furqan M, Song Y and Liu D. Phosphatidylinositol 3-kinase (PI3K) inhibitors as cancer therapeutics. *J Hematol Oncol* 2013; 6: 88.
- [22] Petrilli A, Copik A, Posadas M, Chang LS, Welling DB, Giovannini M and Fernandez-Valle C. LIM domain kinases as potential therapeutic targets for neurofibromatosis type 2. *Oncogene* 2013; 33: 3571-82.
- [23] Thaxton C, Bott M, Walker B, Sparrow NA, Lambert S and Fernandez-Valle C. Schwannomin/merlin promotes Schwann cell elongation and influences myelin segment length. *Mol Cell Neurosci* 2011; 47: 1-9.
- [24] Zhang JH, Chung TD and Oldenburg KR. A Simple Statistical Parameter for Use in Evaluation and Validation of High Throughput Screening Assays. *J Biomol Screen* 1999; 4: 67-73.
- [25] Mayr LM and Bojanic D. Novel trends in high-throughput screening. *Curr Opin Pharmacol* 2009; 9: 580-588.
- [26] Giovannini M, Bonne NX, Vitte J, Chareyre F, Tanaka K, Adams R, Fisher LM, Valeyrie-Allanore L, Wolkenstein P, Goutagny S and Kalamirides M. mTORC1 inhibition delays growth of neurofibromatosis type 2 schwannoma. *Neuro Oncol* 2014; 16: 493-504.
- [27] James MF, Stivison E, Beauchamp R, Han S, Li H, Wallace MR, Gusella JF, Stemmer-Rachamimov AO and Ramesh V. Regulation of

- mTOR complex 2 signaling in neurofibromatosis 2-deficient target cell types. *Mol Cancer Res* 2012; 10: 649-659.
- [28] Klionsky DJ, Abdalla FC, Abeliovich H, Abraham RT, Acevedo-Arozena A, Adeli K, Agholme L, Agnello M, Agostinis P, Aguirre-Ghiso JA, Ahn HJ, Ait-Mohamed O, Ait-Si-Ali S, Akematsu T, Akira S, Al-Younes HM, Al-Zeer MA, Albert ML, Albin RL, Alegre-Abarrategui J, Aleo MF, Alirezaei M, Almasan A, Almonte-Becerril M, Amano A, Amaravadi R, Amarnath S, Amer AO, Andrieu-Abadie N, Anantharam V, Ann DK, Anoopkumar-Dukie S, Aoki H, Apostolova N, Arancia G, Aris JP, Asanuma K, Asare NY, Ashida H, Askanas V, Askew DS, Auberger P, Baba M, Backues SK, Baehrecke EH, Bahr BA, Bai XY, Bailly Y, Baiocchi R, Baldini G, Balduini W, Ballabio A, Bamber BA, Bampton ET, Banhegyi G, Bartholomew CR, Bassham DC, Bast RC, Jr., Batoko H, Bay BH, Beau I, Bechet DM, Begley TJ, Behl C, Behrends C, Bekri S, Bellaire B, Bendall LJ, Benetti L, Berliocchi L, Bernardi H, Bernassola F, Besteiro S, Bhatia-Kissova I, Bi X, Biard-Piechaczyk M, Blum JS, Boise LH, Bonaldo P, Boone DL, Bornhauser BC, Bortoluci KR, Bossis I, Bost F, Bourquin JP, Boya P, Boyer-Guittaut M, Bozhkov PV, Brady NR, Brancolini C, Brech A, Brenman JE, Brennand A, Bresnick EH, Brest P, Bridges D, Bristol ML, Brookes PS, Brown EJ, Brumell JH, Brunetti-Pierri N, Brunk UT, Bulman DE, Bultman SJ, Bultynck G, Burbulla LF, Bursch W, Butchar JP, Buzgariu W, Bydlowski SP, Cadwell K, Cahova M, Cai D, Cai J, Cai Q, Calabretta B, Calvo-Garrido J, Camougrand N, Campanella M, Campos-Salinas J, Candi E, Cao L, Caplan AB, Carding SR, Cardoso SM, Carew JS, Carlin CR, Carmignac V, Carneiro LA, Carra S, Caruso RA, Casari G, Casas C, Castino R, Cebollero E, Cecconi F, Celli J, Chaachouay H, Chae HJ, Chai CY, Chan DC, Chan EY, Chang RC, Che CM, Chen CC, Chen GC, Chen GQ, Chen M, Chen Q, Chen SS, Chen W, Chen X, Chen YG, Chen Y, Chen YJ, Chen Z, Cheng A, Cheng CH, Cheng Y, Cheong H, Cheong JH, Cherry S, Chess-Williams R, Cheung ZH, Chevet E, Chiang HL, Chiarelli R, Chiba T, Chin LS, Chiou SH, Chisari FV, Cho CH, Cho DH, Choi AM, Choi D, Choi KS, Choi ME, Chouaib S, Choubey D, Choubey V, Chu CT, Chuang TH, Chueh SH, Chun T, Chwae YJ, Chye ML, Ciarcia R, Ciriolo MR, Clague MJ, Clark RS, Clarke PG, Clarke R, Codogno P, Collier HA, Colombo MI, Comincini S, Condello M, Condorelli F, Cookson MR, Coombs GH, Coppens I, Corbalan R, Cossart P, Costelli P, Costes S, Coto-Montes A, Couve E, Coxon FP, Cregg JM, Crespo JL, Cronje MJ, Cuervo AM, Cullen JJ, Czaja MJ, D'Amelio M, Darfeuille-Michaud A, Davids LM, Davies FE, De Felici M, de Groot JF, de Haan CA, De Martino L, De Milito A, De Tata V, Debnath J, Degtarev A, Dehay B, Delbridge LM, Demarchi F, Deng YZ, Dengjel J, Dent P, Denton D, Deretic V, Desai SD, Devenish RJ, Di Gioacchino M, Di Paolo G, Di Pietro C, Diaz-Araya G, Diaz-Laviada I, Diaz-Meco MT, Diaz-Nido J, Dikic I, Dinesh-Kumar SP, Ding WX, Distelhorst CW, Diwan A, Djavaheri-Mergny M, Dokudovskaya S, Dong Z, Dorsey FC, Dosenko V, Dowling JJ, Doxsey S, Dreux M, Drew ME, Duan Q, Duchosal MA, Duff K, Dugail I, Durbeeej M, Duszenko M, Edelstein CL, Eninger AL, Egea G, Eichinger L, Eissa NT, Ekmekcioglu S, El-Deiry WS, Elazar Z, Elgendy M, Ellerby LM, Eng KE, Engelbrecht AM, Engelder S, Erenpreisa J, Escalante R, Esclatine A, Eskelinen EL, Espert L, Espina V, Fan H, Fan J, Fan QW, Fan Z, Fang S, Fang Y, Fanto M, Fanzani A, Farkas T, Farre JC, Faure M, Fechheimer M, Feng CG, Feng J, Feng Q, Feng Y, Fesus L, Feuer R, Figueiredo-Pereira ME, Fimia GM, Fingar DC, Finkbeiner S, Finkel T, Finley KD, Fiorito F, Fisher EA, Fisher PB, Flajolet M, Florez-McClure ML, Florio S, Fon EA, Fornai F, Fortunato F, Fotedar R, Fowler DH, Fox HS, Franco R, Frankel LB, Fransen M, Fuentes JM, Fueyo J, Fujii J, Fujisaki K, Fujita E, Fukuda M, Furukawa RH, Gaestel M, Gailly P, Gajewska M, Galliot B, Galy V, Ganesh S, Ganetzky B, Ganley IG, Gao FB, Gao GF, Gao J, Garcia L, Garcia-Manero G, Garcia-Marcos M, Garmyn M, Gartel AL, Gatti E, Gautel M, Gawriluk TR, Gegg ME, Geng J, Germain M, Gestwicki JE, Gewirtz DA, Ghavami S, Ghosh P, Giammarioli AM, Giatromanolaki AN, Gibson SB, Gilkerson RW, Ginger ML, Ginsberg HN, Golab J, Goligorsky MS, Golstein P, Gomez-Manzano C, Goncu E, Gongora C, Gonzalez CD, Gonzalez R, Gonzalez-Esteviz C, Gonzalez-Polo RA, Gonzalez-Rey E, Gorbunov NV, Gorski S, Goruppi S, Gottlieb RA, Gozuacik D, Granato GE, Grant GD, Green KN, Gregorc A, Gros F, Grose C, Grunt TW, Gual P, Guan JL, Guan KL, Guichard SM, Gukovskaya AS, Gukovsky I, Gunst J, Gustafsson AB, Halayko AJ, Hale AN, Halonen SK, Hamasaki M, Han F, Han T, Hancock MK, Hansen M, Harada H, Harada M, Hardt SE, Harper JW, Harris AL, Harris J, Harris SD, Hashimoto M, Haspel JA, Hayashi S, Hazelhurst LA, He C, He YW, Hebert MJ, Heidenreich KA, Helfrich MH, Helgason GV, Henske EP, Herman B, Herman PK, Hetz C, Hilfiker S, Hill JA, Hocking LJ, Hofman P, Hofmann TG, Hohfeld J, Holyoake TL, Hong MH, Hood DA, Hotamisligil GS, Houwerzijl EJ, Hoyer-Hansen M, Hu B, Hu CA, Hu HM, Hua Y, Huang C, Huang J, Huang S, Huang WP, Huber TB, Huh WK, Hung TH, Hupp TR, Hur GM, Hurley JB, Hussain SN, Hussey PJ, Hwang JJ,

PI3K as a pharmacological target in NF2

Hwang S, Ichihara A, Ilkhanizadeh S, Inoki K, Into T, Iovane V, Iovanna JL, Ip NY, Isaka Y, Ishida H, Isidoro C, Isobe K, Iwasaki A, Izquierdo M, Izumi Y, Jaakkola PM, Jaattela M, Jackson GR, Jackson WT, Janji B, Jendrach M, Jeon JH, Jeung EB, Jiang H, Jiang JX, Jiang M, Jiang Q, Jiang X, Jimenez A, Jin M, Jin S, Joe CO, Johansen T, Johnson DE, Johnson GV, Jones NL, Joseph B, Joseph SK, Joubert AM, Juhasz G, Juillerat-Jeanneret L, Jung CH, Jung YK, Kaarniranta K, Kaasik A, Kabuta T, Kadowaki M, Kagedal K, Kamada Y, Kaminsky VO, Kampinga HH, Kanamori H, Kang C, Kang KB, Kang KI, Kang R, Kang YA, Kanki T, Kanneganti TD, Kanno H, Kanthasamy AG, Kanthasamy A, Karantza V, Kaushal GP, Kaushik S, Kawazoe Y, Ke PY, Kehrl JH, Kelekar A, Kerkhoff C, Kessel DH, Khalil H, Kiel JA, Kiger AA, Kihara A, Kim DR, Kim DH, Kim EK, Kim HR, Kim JS, Kim JH, Kim JC, Kim JK, Kim PK, Kim SW, Kim YS, Kim Y, Kimchi A, Kimmelman AC, King JS, Kinsella TJ, Kirkin V, Kirshenbaum LA, Kitamoto K, Kitazato K, Klein L, Klimecki WT, Klucken J, Knecht E, Ko BC, Koch JC, Koga H, Koh JY, Koh YH, Koike M, Komatsu M, Kominami E, Kong HJ, Kong WJ, Korolchuk VI, Kotake Y, Koukourakis MI, Kouri Flores JB, Kovacs AL, Kraft C, Krainc D, Kramer H, Kretz-Remy C, Krichevsky AM, Kroemer G, Kruger R, Krut O, Ktistakis NT, Kuan CY, Kucharczyk R, Kumar A, Kumar R, Kumar S, Kundu M, Kung HJ, Kurz T, Kwon HJ, La Spada AR, Lafont F, Lamark T, Landry J, Lane JD, Lapaquette P, Laporte JF, Laszlo L, Lavandero S, Lavoie JN, Layfield R, Lazo PA, Le W, Le Cam L, Ledbetter DJ, Lee AJ, Lee BW, Lee GM, Lee J, Lee JH, Lee M, Lee MS, Lee SH, Leeuwenburgh C, Legembre P, Legouis R, Lehmann M, Lei HY, Lei QY, Leib DA, Leiro J, Lemasters JJ, Lemoine A, Lesniak MS, Lev D, Levenson VV, Levine B, Levy E, Li F, Li JL, Li L, Li S, Li W, Li XJ, Li YB, Li YP, Liang C, Liang Q, Liao YF, Liberski PP, Lieberman A, Lim HJ, Lim KL, Lim K, Lin CF, Lin FC, Lin J, Lin JD, Lin K, Lin WW, Lin WC, Lin YL, Linden R, Lingor P, Lippincott-Schwartz J, Lisanti MP, Liton PB, Liu B, Liu CF, Liu K, Liu L, Liu QA, Liu W, Liu YC, Liu Y, Lockshin RA, Lok CN, Lonial S, Loos B, Lopez-Berestein G, Lopez-Otin C, Lossi L, Lotze MT, Low P, Lu B, Lu Z, Luciano F, Lukacs NW, Lund AH, Lynch-Day MA, Ma Y, Macian F, MacKeigan JP, Macleod KF, Madeo F, Maiuri L, Maiuri MC, Malagoli D, Malicdan MC, Malorni W, Man N, Mandelkow EM, Manon S, Manov I, Mao K, Mao X, Mao Z, Marambaud P, Marazziti D, Marcel YL, Marchbank K, Marchetti P, Marciniak SJ, Marcondes M, Mardi M, Marfe G, Marino G, Markaki M, Marten MR, Martin SJ, Martinand-Mari C, Martinet W, Martinez-Vicente M, Masini M, Matarrese P, Matsuo S, Matteoni R, Mayer A, Mazure NM, McConkey DJ, McConnell MJ, McDermott C, McDonald C, McInerney GM, McKenna SL, McLaughlin B, McLean PJ, McMaster CR, McQuibban GA, Meijer AJ, Meisler MH, Melendez A, Melia TJ, Melino G, Mena MA, Menendez JA, Menna-Barreto RF, Menon MB, Menzies FM, Mercer CA, Merighi A, Merry DE, Meschini S, Meyer CG, Meyer TF, Miao CY, Miao JY, Michels PA, Michiels C, Mijaljica D, Milojkovic A, Minucci S, Miracco C, Miranti CK, Mitroulis I, Miyazawa K, Mizushima N, Mograbi B, Mohseni S, Molero X, Mollereau B, Mollinedo F, Momoi T, Monastyrska I, Monick MM, Monteiro MJ, Moore MN, Mora R, Moreau K, Moreira PI, Moriyasu Y, Moscat J, Mostow S, Mottram JC, Motyl T, Moussa CE, Muller S, Munger K, Munz C, Murphy LO, Murphy ME, Musaro A, Mysorekar I, Nagata E, Nagata K, Nahimana A, Nair U, Nakagawa T, Nakahira K, Nakano H, Nakatogawa H, Nanjundan M, Naqvi NI, Narendra DP, Narita M, Navarro M, Nawrocki ST, Nazarko TY, Nemchenko A, Netea MG, Neufeld TP, Ney PA, Nezis IP, Nguyen HP, Nie D, Nishino I, Nislow C, Nixon RA, Noda T, Noegel AA, Nogalska A, Noguchi S, Notterpek L, Novak I, Nozaki T, Nukina N, Nurnberger T, Nyfeler B, Obara K, Oberley TD, Oddo S, Ogawa M, Ohashi T, Okamoto K, Oleinick NL, Oliver FJ, Olsen LJ, Olsson S, Opota O, Osborne TF, Ostrander GK, Otsu K, Ou JH, Ouimet M, Overholtzer M, Ozpolat B, Paganetti P, Pagnini U, Pallet N, Palmer GE, Palumbo C, Pan T, Panaretakis T, Pandey UB, Papackova Z, Papassideri I, Paris I, Park J, Park OK, Parys JB, Parzych KR, Patschan S, Patterson C, Pattingre S, Pawelek JM, Peng J, Perlmutter DH, Perrotta I, Perry G, Pervaiz S, Peter M, Peters GJ, Petersen M, Petrovski G, Phang JM, Piacentini M, Pierre P, Pierrefite-Carle V, Pierron G, Pinkas-Kramarski R, Piras A, Piri N, Platanias LC, Poggeler S, Poirot M, Poletti A, Pous C, Pozuelo-Rubio M, Praetorius-Ibba M, Prasad A, Prescott M, Priault M, Produit-Zengaffinen N, Progulske-Fox A, Proikas-Cezanne T, Przedborski S, Przyklenk K, Puertollano R, Puyal J, Qian SB, Qin L, Qin ZH, Quaggin SE, Raben N, Rabinowich H, Rabkin SW, Rahman I, Rami A, Ramm G, Randall G, Randow F, Rao VA, Rathmell JC, Ravikumar B, Ray SK, Reed BH, Reed JC, Reggiori F, Regnier-Vigouroux A, Reichert AS, Reiners JJ, Jr., Reiter RJ, Ren J, Revuelta JL, Rhodes CJ, Ritis K, Rizzo E, Robbins J, Roberge M, Roca H, Roccheri MC, Rocchi S, Rodemann HP, Rodriguez de Cordoba S, Rohrer B, Roninson IB, Rosen K, Rost-Roszkowska MM, Rouis M, Rouschop KM, Rovetta F, Rubin BP, Rubinsztein DC, Ruckdeschel K, Rucker EB, 3rd, Rudich A, Rudolf E, Ruiz-Opazo N, Russo

- R, Rusten TE, Ryan KM, Ryter SW, Sabatini DM, Sadoshima J, Saha T, Saitoh T, Sakagami H, Sakai Y, Salekdeh GH, Salomoni P, Salvaterra PM, Salvesen G, Salvioli R, Sanchez AM, Sanchez-Alcazar JA, Sanchez-Prieto R, Sandri M, Sankar U, Sansanwal P, Santambrogio L, Saran S, Sarkar S, Sarwal M, Sasakawa C, Sasnauskiene A, Sass M, Sato K, Sato M, Schapira AH, Scharl M, Schatzl HM, Scheper W, Schiaffino S, Schneider C, Schneider ME, Schneider-Stock R, Schoenlein PV, Schorderet DF, Schuller C, Schwartz GK, Scorrano L, Sealy L, Seglen PO, Segura-Aguilar J, Seiliez I, Seleverstov O, Sell C, Seo JB, Separovic D, Setaluri V, Setoguchi T, Settembre C, Shacka JJ, Shanmugam M, Shapiro IM, Shaulian E, Shaw RJ, Shelhamer JH, Shen HM, Shen WC, Sheng ZH, Shi Y, Shibuya K, Shidoji Y, Shieh JJ, Shih CM, Shimada Y, Shimizu S, Shintani T, Shirihai OS, Shore GC, Sibirny AA, Sidhu SB, Sikorska B, Silva-Zacarin EC, Simmons A, Simon AK, Simon HU, Simone C, Simonsen A, Sinclair DA, Singh R, Sinha D, Sinicrope FA, Sirko A, Siu PM, Sivridis E, Skop V, Skulachev VP, Slack RS, Smaili SS, Smith DR, Soengas MS, Soldati T, Song X, Sood AK, Soong TW, Sotgia F, Spector SA, Spies CD, Springer W, Srinivasula SM, Stefanis L, Steffan JS, Stendel R, Stenmark H, Stephanou A, Stern ST, Sternberg C, Stork B, Stralfors P, Subauste CS, Sui X, Sulzer D, Sun J, Sun SY, Sun ZJ, Sung JJ, Suzuki K, Suzuki T, Swanson MS, Swanton C, Sweeney ST, Sy LK, Szabadkai G, Tabas I, Taegtmeier H, Tafani M, Takacs-Vellai K, Takano Y, Takegawa K, Takemura G, Takeshita F, Talbot NJ, Tan KS, Tanaka K, Tang D, Tanida I, Tannous BA, Tavernarakis N, Taylor GS, Taylor GA, Taylor JP, Terada LS, Terman A, Tettamanti G, Thevissen K, Thompson CB, Thorburn A, Thumm M, Tian F, Tian Y, Tocchini-Valentini G, Tolkovsky AM, Tomino Y, Tonges L, Tooze SA, Tournier C, Tower J, Towns R, Trajkovic V, Travassos LH, Tsai TF, Tschan MP, Tsubata T, Tsung A, Turk B, Turner LS, Tyagi SC, Uchiyama Y, Ueno T, Umekawa M, Umemiya-Shirafuji R, Unni VK, Vaccaro MI, Valente EM, Van den Berghe G, van der Klei IJ, van Doorn W, van Dyk LF, van Egmond M, van Grunsven LA, Vandenabeele P, Vandenbergh WP, Vanhorebeek I, Vaquero EC, Velasco G, Vellai T, Vicencio JM, Vierstra RD, Vila M, Vindis C, Viola G, Viscomi MT, Voitsekhovskaja OV, von Haefen C, Votruba M, Wada K, Wade-Martins R, Walker CL, Walsh CM, Walter J, Wan XB, Wang A, Wang C, Wang D, Wang F, Wang G, Wang H, Wang HG, Wang HD, Wang J, Wang K, Wang M, Wang RC, Wang X, Wang YJ, Wang Y, Wang Z, Wang ZC, Wansink DG, Ward DM, Watada H, Waters SL, Webster P, Wei L, Wehl CC, Weiss WA, Welford SM, Wen LP, Whitehouse CA, Whitton JL, Whitworth AJ, Wileman T, Wiley JW, Wilkinson S, Willbold D, Williams RL, Williamson PR, Wouters BG, Wu C, Wu DC, Wu WK, Wyttenbach A, Xavier RJ, Xi Z, Xia P, Xiao G, Xie Z, Xu DZ, Xu J, Xu L, Xu X, Yamamoto A, Yamashina S, Yamashita M, Yan X, Yanagida M, Yang DS, Yang E, Yang JM, Yang SY, Yang W, Yang WY, Yang Z, Yao MC, Yao TP, Yeganeh B, Yen WL, Yin JJ, Yin XM, Yoo OJ, Yoon G, Yoon SY, Yorimitsu T, Yoshikawa Y, Yoshimori T, Yoshimoto K, You HJ, Youle RJ, Younes A, Yu L, Yu SW, Yu WH, Yuan ZM, Yue Z, Yun CH, Yuzaki M, Zabirnyk O, Silva-Zacarin E, Zacks D, Zacksenhaus E, Zaffaroni N, Zakeri Z, Zeh HJ, 3rd, Zeitlin SO, Zhang H, Zhang HL, Zhang J, Zhang JP, Zhang L, Zhang MY, Zhang XD, Zhao M, Zhao YF, Zhao Y, Zhao ZJ, Zheng X, Zhivotovsky B, Zhong Q, Zhou CZ, Zhu C, Zhu WG, Zhu XF, Zhu X, Zhu Y, Zoladek T, Zong WX, Zorzano A, Zschocke J and Zuckerbraun B. Guidelines for the use and interpretation of assays for monitoring autophagy. *Autophagy* 2012; 8: 445-544.
- [29] Sadhu C, Masinovsky B, Dick K, Sowell CG and Staunton DE. Essential role of phosphoinositide 3-kinase delta in neutrophil directional movement. *J Immunol* 2003; 170: 2647-2654.
- [30] Petrilli A, Bott M and Fernandez-Valle C. Inhibition of SIRT2 in merlin/NF2-mutant Schwann cells triggers necrosis. *Oncotarget* 2013; 4: 2354-2365.
- [31] Graziano MJ and Casida JE. Comparison of the acute toxicity of endothal and cantharidic acid on mouse liver in vivo. *Toxicol Lett* 1987; 37: 143-148.
- [32] Camps M, Ruckle T, Ji H, Ardisson V, Rintelen F, Shaw J, Ferrandi C, Chabert C, Gillieron C, Francon B, Martin T, Gretener D, Perrin D, Leroy D, Vitte PA, Hirsch E, Wymann MP, Cirillo R, Schwarz MK and Rommel C. Blockade of PI3Kgamma suppresses joint inflammation and damage in mouse models of rheumatoid arthritis. *Nat Med* 2005; 11: 936-943.
- [33] Mielcke TR, Mascarello A, Filippi-Chiela E, Zanin RF, Lenz G, Leal PC, Chiaradia LD, Nunes RA, Nunes RJ, Battastini AM, Morrone FB and Campos MM. Activity of novel quinoxaline-derived chalcones on in vitro glioma cell proliferation. *Eur J Med Chem* 2012; 48: 255-264.
- [34] Spitzenberg V, Konig C, Ulm S, Marone R, Ropke L, Muller JP, Grun M, Bauer R, Rubio I, Wymann MP, Voigt A and Wetzker R. Targeting PI3K in neuroblastoma. *J Cancer Res Clin Oncol* 2010; 136: 1881-1890.

PI3K as a pharmacological target in NF2

- [35] Duronio V. The life of a cell: apoptosis regulation by the PI3K/PKB pathway. *Biochem J* 2008; 415: 333-344.
- [36] Lallemand D, Manent J, Couvelard A, Watilliaux A, Siena M, Chareyre F, Lampin A, Niwa-Kawakita M, Kalamarides M and Giovannini M. Merlin regulates transmembrane receptor accumulation and signaling at the plasma membrane in primary mouse Schwann cells and in human schwannomas. *Oncogene* 2009; 28: 854-865.
- [37] Li Y, Tennekoon GI, Birnbaum M, Marchionni MA and Rutkowski JL. Neuregulin signaling through a PI3K/Akt/Bad pathway in Schwann cell survival. *Mol Cell Neurosci* 2001; 17: 761-767.
- [38] Folkes AJ, Ahmadi K, Alderton WK, Alix S, Baker SJ, Box G, Chuckowree IS, Clarke PA, Depledge P, Eccles SA, Friedman LS, Hayes A, Hancox TC, Kugendradas A, Lensun L, Moore P, Olivero AG, Pang J, Patel S, Pergl-Wilson GH, Raynaud FI, Robson A, Saghir N, Salphati L, Sohal S, Ultsch MH, Valenti M, Wallweber HJ, Wan NC, Wiesmann C, Workman P, Zhyvoloup A, Zvelebil MJ and Shuttleworth SJ. The identification of 2-(1H-indazol-4-yl)-6-(4-methanesulfonylpiperazin-1-ylmethyl)-4-morpholin-4-yl-thieno[3,2-d]pyrimidine (GDC-0941) as a potent, selective, orally bioavailable inhibitor of class I PI3 kinase for the treatment of cancer. *J Med Chem* 2008; 51: 5522-5532.
- [39] Ohwada J, Ebiike H, Kawada H, Tsukazaki M, Nakamura M, Miyazaki T, Morikami K, Yoshinari K, Yoshida M, Kondoh O, Kuramoto S, Ogawa K, Aoki Y and Shimma N. Discovery and biological activity of a novel class I PI3K inhibitor, CH5132799. *Bioorg Med Chem Lett* 2011; 21: 1767-1772.
- [40] Talekar M, Ganta S, Singh A, Amiji M, Kendall J, Denny WA and Garg S. Phosphatidylinositol 3-kinase inhibitor (PIK75) containing surface functionalized nanoemulsion for enhanced drug delivery, cytotoxicity and pro-apoptotic activity in ovarian cancer cells. *Pharm Res* 2012; 29: 2874-2886.
- [41] Tanaka H, Yoshida M, Tanimura H, Fujii T, Sakata K, Tachibana Y, Ohwada J, Ebiike H, Kuramoto S, Morita K, Yoshimura Y, Yamazaki T, Ishii N, Kondoh O and Aoki Y. The selective class I PI3K inhibitor CH5132799 targets human cancers harboring oncogenic PIK3CA mutations. *Clin Cancer Res* 2011; 17: 3272-3281.
- [42] Cloughesy TF, Yoshimoto K, Nghiemphu P, Brown K, Dang J, Zhu S, Hsueh T, Chen Y, Wang W, Youngkin D, Liao L, Martin N, Becker D, Bergsneider M, Lai A, Green R, Oglesby T, Koleto M, Trent J, Horvath S, Mischel PS, Mellinghoff IK and Sawyers CL. Antitumor activity of rapamycin in a Phase I trial for patients with recurrent PTEN-deficient glioblastoma. *PLoS Med* 2008; 5: e8.
- [43] Liu P, Cheng H, Roberts TM and Zhao JJ. Targeting the phosphoinositide 3-kinase pathway in cancer. *Nat Rev Drug Discov* 2009; 8: 627-644.
- [44] Maira SM, Stauffer F, Schnell C and Garcia-Echeverria C. PI3K inhibitors for cancer treatment: where do we stand? *Biochem Soc Trans* 2009; 37: 265-272.
- [45] Leung E, Kim JE, Rewcastle GW, Finlay GJ and Baguley BC. Comparison of the effects of the PI3K/mTOR inhibitors NVP-BEZ235 and GSK2126458 on tamoxifen-resistant breast cancer cells. *Cancer Biol Ther* 2011; 11: 938-946.
- [46] Qian C, Lai CJ, Bao R, Wang DG, Wang J, Xu GX, Atayan R, Qu H, Yin L, Samson M, Zifcak B, Ma AW, DellaRocca S, Borek M, Zhai HX, Cai X and Voi M. Cancer network disruption by a single molecule inhibitor targeting both histone deacetylase activity and phosphatidylinositol 3-kinase signaling. *Clin Cancer Res* 2012; 18: 4104-4113.

PI3K as a pharmacological target in NF2

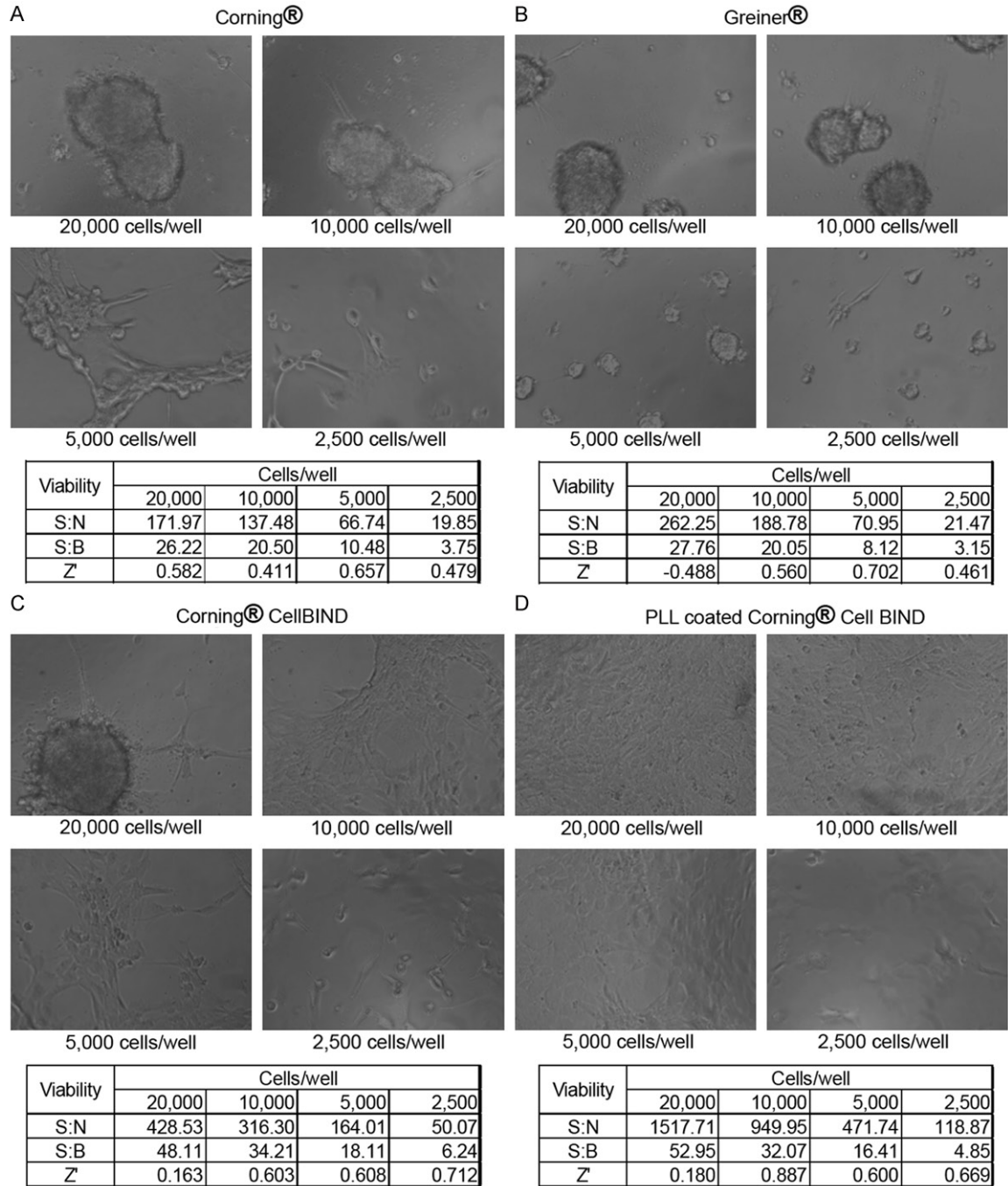
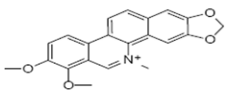
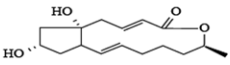
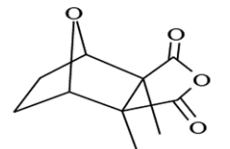
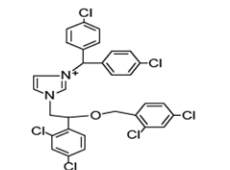
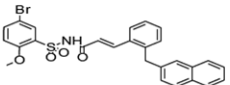
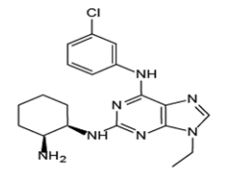
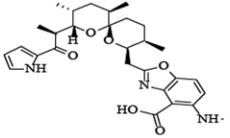
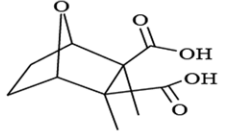
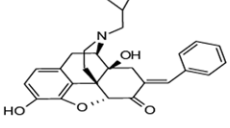
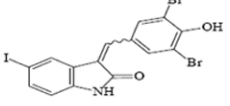
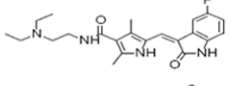
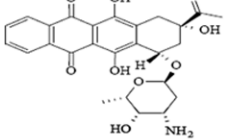
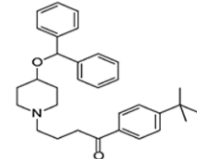
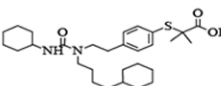
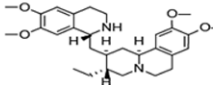
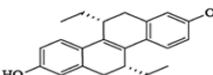
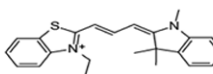
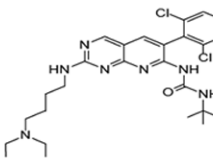
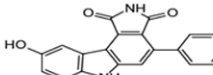
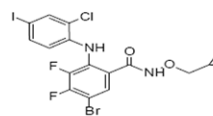
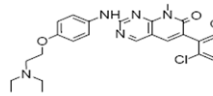
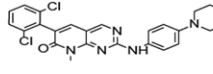
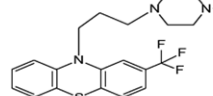
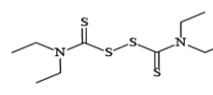
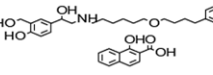
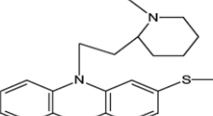


Figure S1. Optimal Merlin-null MSC Density at Seeding and Plate Performance. Phase contrast images of merlin-null MSCs seeded from 2,500 cells/well to 20,000 cells/well after 24 hrs incubation with the quality control parameter determined with a fluorescence viability assay. (A) Corning, (B) Greiner, (C) Corning CellBIND, and (D) PLL-coated Corning 384-well plate.

PI3K as a pharmacological target in NF2

CompoundID	Structure	BatchID	Compound Vendor	Vendor Compound ID	Percent Efficacy	Comments
SBI-0050229		SBI-0050229.P004	Sigma-Aldrich	C 2932	85.503	PKC inhibitor; affects translocation of PKC from cytosol to plasma membrane
SBI-0050152		SBI-0050152.P003	Sigma-Aldrich	B 7651	95.922	Fungal metabolite that disrupts the structure and function of the Golgi apparatus
SBI-0050236		SBI-0050236.P003	Sigma-Aldrich	C 7632	99.734	Protein phosphatase 2A inhibitor
SBI-0050260		SBI-0050260.P004	Sigma-Aldrich	C 3930	97.072	Potent inhibitor of calmodulin activation of phosphodiesterase; strongly inhibits calmodulin-dependent Ca ²⁺ -ATPase
SBI-0635801		SBI-0635801.P001	Sigma-Aldrich	L4545	94.771	L-798106 L-798106 was among the first EP3-selective antagonists
SBI-0050279		SBI-0050279.P004	Sigma-Aldrich	C 3353	100.42	Cdk1 inhibitor
SBI-0050305		SBI-0050305.P003	Sigma-Aldrich	C 7522	93.983	Ca ²⁺ ionophore used to potentiate responses to NMDA, but not quisqualate glutamate receptors
SBI-0050306		SBI-0050306.P003	Sigma-Aldrich	C 8088	100.16	Protein phosphatase 1 (PP1) and 2A (PP2A) inhibitor
SBI-0633734		SBI-0633734.P002	Sigma-Aldrich	B 8312	94.481	BNTX is a selective d1 non peptide opioid receptor antagonist. BNTX is used as a tool for the study of various function of opioid receptors including alcohol and drug dependence
SBI-0050494		SBI-0050494.P003	Sigma-Aldrich	G 6416	83.363	cRaf1 kinase inhibitor
SBI-0634415		SBI-0634415.P002	Sigma-Aldrich	PZ0012	91.07	Sunitinib (free base)
SBI-0050582		SBI-0050582.P004	Sigma-Aldrich	I 1656	99.269	Antineoplastic

PI3K as a pharmacological target in NF2

SBI-0633701		SBI-0633701.P002	Sigma-Aldrich	E9531	95.826	Nonsedating histamine H1 receptor antagonist without cardiac side effects at 5X effective dose.
SBI-0050513		SBI-0050513.P003	Sigma-Aldrich	G 6793	95.826	Potent agonist of peroxisome proliferator-activated alpha (PPAR-alpha)
SBI-0050445		SBI-0050445.P003	Sigma-Aldrich	E 2375	99.433	Apoptosis inducer; RNA-Protein translation inhibitor
SBI-0050448		SBI-0050448.P003	Sigma-Aldrich	D 8690	98.646	Potent estrogen receptor beta antagonist; potent partial agonist at estrogen receptor alpha
SBI-0633717		SBI-0633717.P002	Sigma-Aldrich	A9605	84.248	Potent, cell permeable, subtype selective retinoic acid receptor (RARalpha) agonist.
SBI-0635826		SBI-0635826.P001	Sigma-Aldrich	PZ0109	94.464	PD-161570 PD-161570 is an inhibitor of human FGF-1 receptor tyrosine kinase.
SBI-0207207		SBI-0207207.P002	Sigma-Aldrich	PZ0111	81.129	Wee1/Chk1 Inhibitor
SBI-0635840		SBI-0635840.P001	Sigma-Aldrich	PZ0112	91.072	PD-184161 PD-184161 is a MEK inhibitor.
SBI-0635850		SBI-0635850.P001	Sigma-Aldrich	PZ0116	100.79	PD-166285 hydrate PD-166285 hydrate is a broad spectrum protein tyrosine kinase inhibitor; Src and FGFR kinase inhibitor
SBI-0635843		SBI-0635843.P001	Sigma-Aldrich	PZ0113	92.87	PD173952 PD173952 is a Src family kinase inhibitor.
SBI-0051199		SBI-0051199.P007	Sigma-Aldrich	T 8516	86.473	Calmodulin antagonist; dopamine receptor antagonist; antipsychotic; sedative
SBI-0051131		SBI-0051131.P007	Sigma-Aldrich	T 1132	95.083	Alcohol dehydrogenase inhibitor
SBI-0633788		SBI-0633788.P002	Sigma-Aldrich	S 5068	88.133	beta2 Adrenoceptor agonist
SBI-0051219		SBI-0051219.P006	Sigma-Aldrich	T 9025	90.173	Dopamine receptor antagonist; Ca2+ channel antagonist; antipsychotic

PI3K as a pharmacological target in NF2

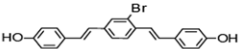
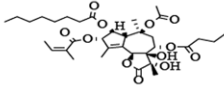
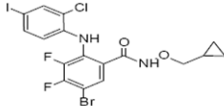
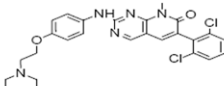
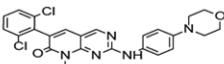
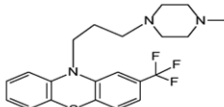
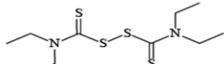
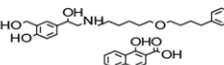
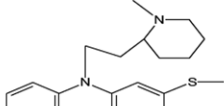
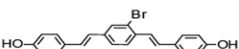
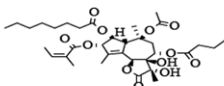
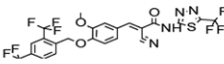
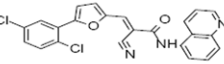
SBI-0633777		SBI-0633777.P002	Sigma-Aldrich	K 1015	89.862	A fluorescent, amyloid-specific dye, an analogue of Congo Red and BSB that recognizes amyloid lesions and allows the quantitative monitoring of the formation of amyloid fibrils assembled from the Aβ peptide, a-synuclein, and tau.
SBI-0051229		SBI-0051229.P004	Sigma-Aldrich	T 9033	94.288	Potent, cell-permeable, IP3-independent intracellular calcium releaser
SBI-0635840		SBI-0635840.P001	Sigma-Aldrich	PZ0112	91.072	PD-184161 PD-184161 is a MEK inhibitor.
SBI-0635850		SBI-0635850.P001	Sigma-Aldrich	PZ0116	100.79	PD-166285 hydrate PD-166285 hydrate is a broad spectrum protein tyrosine kinase inhibitor; Src and FGFR kinase inhibitor
SBI-0635843		SBI-0635843.P001	Sigma-Aldrich	PZ0113	92.87	PD173952 PD173952 is a Src family kinase inhibitor.
SBI-0051199		SBI-0051199.P007	Sigma-Aldrich	T 8516	86.473	Calmodulin antagonist; dopamine receptor antagonist; antipsychotic; sedative
SBI-0051131		SBI-0051131.P007	Sigma-Aldrich	T 1132	95.083	Alcohol dehydrogenase inhibitor
SBI-0633788		SBI-0633788.P002	Sigma-Aldrich	S 5068	88.133	beta2 Adrenoceptor agonist
SBI-0051219		SBI-0051219.P006	Sigma-Aldrich	T 9025	90.173	Dopamine receptor antagonist; Ca2+ channel antagonist; antipsychotic
SBI-0633777		SBI-0633777.P002	Sigma-Aldrich	K 1015	89.862	A fluorescent, amyloid-specific dye, an analogue of Congo Red and BSB that recognizes amyloid lesions and allows the quantitative monitoring of the formation of amyloid fibrils assembled from the Aβ peptide, a-synuclein, and tau.
SBI-0051229		SBI-0051229.P004	Sigma-Aldrich	T 9033	94.288	Potent, cell-permeable, IP3-independent intracellular calcium releaser
SBI-0633819		SBI-0633819.P002	Sigma-Aldrich	X4753	93.112	Potent and selective estrogen-related receptor alpha (ERRalpha)
SBI-0633793		SBI-0633793.P003	Sigma-Aldrich	A 8231	90.207	SIRT2 inhibitor. AGK2 rescues dopamine neurons from a-synuclein toxicity in Parkinson's disease models.

Figure S2. Complete List of Hits from the LOPAC Screen in Merlin-Null MSCs.